Quasiparticles and vortices in unconventional superconductors

O. Vafek, A. Melikyan, M. Franz,* and Z. Tešanović
Department of Physics and Astronomy, Johns Hopkins University, Baltimore, Maryland 21218
(Received 20 July 2000; published 7 March 2001)

Quasiparticles in the vortex lattice of strongly type-II superconductors are investigated by means of a singular gauge transformation applied to the tight-binding lattice Bogoliubov-de Gennes Hamiltonian. We present a detailed derivation of the gauge invariant effective low-energy Hamiltonian for the quasiparticle-vortex system and show how the physics of the ''Doppler shift'' and ''Berry phase'' can be incorporated at the Hamiltonian level by working in the singular gauge. In particular, we show that the ''Berry phase'' effect manifests itself in the effective Hamiltonian through a half-flux Aharonov-Bohm scattering of quasiparticles off vortices and stress the important role that this effect plays in the quasiparticle dynamics. Full numerical solutions in the regime of intermediate fields $H_{c1} \ll B \ll H_{c2}$ are presented for model superconductors with *s*-, *p*-, and *d*-wave symmetries and with square and triangular vortex lattices. For *s*- and *p*-wave cases we obtain low-energy bound states in the core, in agreement with the existing results. For the *d*-wave case only extended quasiparticle states exist. We investigate in detail the nature of these extended states and provide comparison to the previous results within linearized ''Dirac fermion'' model. We also investigate internodal interference effects when vortex and ionic lattices have a high degree of commensurability and discuss various specific choices for the singular gauge transformation.

DOI: 10.1103/PhysRevB.63.134509 PACS number(s): 74.60.Ec, 74.72.−h

I. INTRODUCTION

In conventional (*s*-wave) superconductors the single-particle fermionic excitations (quasiparticles) are fully gapped everywhere on the Fermi surface and the quasiparticle density of states vanishes below a specific energy. This has profound consequences for the traditional phenomenology of superconductors. The gap in the fermionic spectrum leads to the well-known activated BCS form of the quasiparticle contribution to various thermodynamic and transport properties. Furthermore, even as one moves beyond the mean-field BCS theory, the absence of low-energy quasiparticles in the superconducting state allows one to rewrite the problem of superconducting fluctuations as a ''bosonic'' theory, with the role of bosons played by fluctuating Cooper pairs, after integrating out ''fermionic'' degrees of freedom, i.e., the quasiparticles. In high-temperature superconductors (HTS), however, everything is different: the cuprates appear to be accurately described by the $d_{x^2-y^2}$-wave order parameter,[1] consequently allowing quasiparticle excitations at arbitrary low-energy near the nodal points. These low-energy fermionic excitations appear to govern much of the thermodynamics and transport in the HTS materials. We are thus handed a new intellectual challenge:[2] we must devise methods that can incorporate the low-energy fermionic excitations into the phenomenology of superconductors, both within the mean-field BCS-like theory and beyond.

This challenge is not trivial and has many diverse components: low-energy quasiparticles are scattered by impurities in unusual ways, depending on the low-energy density of states;[3] they interact with external perturbations in ways not encountered in conventional superconductors and these interactions give rise to unusual phenomena;[4,5] the low-energy quasiparticles are expected to qualitatively affect the quantum critical behavior of HTS. Among many aspects of this quasiparticle phenomenology a particularly prominent role is played by the low-lying quasiparticle excitations in the mixed (or vortex) state. All HTS are extreme type-II systems and have a huge mixed phase extending from the lower critical field H_{c1} which is in the range of 10–100 G to the upper critical field H_{c2} which can be as large as 100–200 T. We suspect that in this large region the interactions between quasiparticles and vortices play the essential role in defining the nature of thermodynamic and transport properties.

Such thermodynamic and transport properties are expected to be rather different for distinct classes of unconventional superconductors. This difference stems from a complex motion of the quasiparticles under the combined effects of both the magnetic field **B** and the local drift produced by chiral supercurrents of the vortex state. For example, in HTS the $d_{x^2-y^2}$-wave nature of the gap function results in its vanishing along nodal directions. Along these nodal directions the pair breaking induced by supercurrents has a particularly strong effect. On the other hand, in unconventional superconductors with the $p_{x\pm iy}$ pairing, Sr_2RuO_4 being a possible candidate,[6] the spectrum is fully gapped but the order parameter is chiral even in the absence of external magnetic field. This leads to two different types of vortices for two different field orientations.[7,8]

Still, in all these different situations, the quantum dynamics of quasiparticles in the vortex state contains two essential common ingredients. *First*, there is a purely classical effect of a Doppler shift:[4,5] a quasiparticle energy is shifted by a locally drifting superfluid, $E(\mathbf{k}) \rightarrow E(\mathbf{k}) - \hbar \mathbf{v}_s(\mathbf{r}) \cdot \mathbf{k}$, where $\mathbf{v}_s(\mathbf{r})$ is the local superfluid velocity. $\mathbf{v}_s(\mathbf{r})$ contains information about vortex configurations allowing us to connect quasiparticle spectral properties to various cooperative phenomena in the system of vortices.[9–11] The Doppler shift effect is not peculiar to the vortex state. It also occurs in the Meissner phase[5] and is generally present whenever a quasiparticle experiences a locally uniform drift in the superfluid velocity. *Second*, there is also a purely quantum effect which is inti-

mately tied to the vortex state: as a quasiparticle circles around a vortex while maintaining its quantum coherence, the accumulated phase through a Doppler shift is $\pm\pi$. This implies that there must be an *additional* compensating $\pm\pi$ contribution to the phase on top of the one due to the Doppler shift.[12] The required $\pm\pi$ contribution is supplied by a ''Berry phase'' effect and can be built in at the Hamiltonian level as a half-flux Aharonov-Bohm scattering of quasiparticles by vortices.[12] This interplay between the classical (Doppler shift) and purely quantum effect (''Berry phase'') is what makes the problem of quasiparticle-vortex interaction particularly fascinating.

Let us briefly review what is already known about the subject. The initial theoretical investigations of gapped and gapless superconductors in the vortex state were directed along rather separate lines. The low-energy quasiparticle spectrum of an *s*-wave superconductor in the mixed state was originally studied by Caroli, de Gennes, and Matricon (CdGM)[13] within the framework of the Bogoliubov-de Gennes equations.[14] Their solution yields well-known bound states in the vortex cores. These states are *localized* in the core and have an exponential envelope the scale of which is set by the BCS coherence length. The low-energy end of the spectrum is given by $\epsilon_\mu \sim \mu(\Delta_0^2/E_F)$, where $\mu = 1/2, 3/2, \ldots$, Δ_0 is the overall BCS gap and E_F is the Fermi energy. This solution can be relatively straightforwardly generalized to a fully *gapped*, *chiral p*-wave superconductor. In this case the low-energy quasiparticle spectrum also displays bound vortex core states, whose energy quantization is, however, modified relative to its *s*-wave counterpart, precisely because of the chiral character of a $p_{x\pm iy}$-wave superconductor and the ensuing shift in the angular momentum. For example, the low-energy spectrum of quasiparticles in the singly quantized vortex of the $p_{x\pm iy}$-wave superconductor, possesses a state at exactly zero energy.[7,8]

By comparison, the spectrum of a *gapless d*-wave superconductor in the mixed phase has become the subject of an active debate only relatively recently, fueled by the interest in HTS. Naturally, the first question that arises is what is the analog of the CdGM solution for a single vortex? It is important to realize here that the situation in a $d_{x^2-y^2}$ superconductor is *qualitatively different* from the classic *s*-wave case:[15] when the pairing state has a finite angular momentum and is not a global eigenstate of the angular momentum L_z (a $d_{x^2-y^2}$ superconductor is an equal admixture of $L_z = \pm 1$ states), the problem of fermionic excitations in the core *cannot* be reduced to a collection of decoupled one-dimensional (1D) dimensional eigenvalue equations for each angular momentum channel, the key feature of the CdGM solution. Instead, all channels remain coupled and one must solve a *full* 2D problem. The fully self-consistent numerical solution of the BdG equations[15,16] reveals the most important physical consequence of this qualitatively new situation: the vortex core quasiparticle states in a pure $d_{x^2-y^2}$ superconductor are *delocalized* with wave functions extended along the nodal directions. The low-lying states have a continuous spectrum and, in a broad range of parameters, do not seem to exhibit strong resonant behavior. Obviously, this is in sharp contrast with a discrete spectrum and true bound quasiparticle states of the CdGM *s*-wave solution. We expect the above qualitative results to hold for all unconventional superconductors and within confines of the simple BdG equations, as long as there are nodes in the gap.

A particularly important issue in this context is the nature of the quasiparticle excitations at very low fields, in the presence of a vortex lattice. This is a challenge since the spectrum starts as gapless at zero field and at issue is the interaction of these low-lying quasiparticles with the vortex lattice. This problem has been addressed via a numerical solution of the tight-binding model,[17] a numerical diagonalization of the continuum model[18] and a semiclassical analysis.[4] Gorkov, Schrieffer[19] and, in a somewhat different context, Anderson,[20] predicted that the quasiparticle spectrum is described by a Dirac-like Landau quantization of energy levels

$$E_n = \pm \hbar \omega_H \sqrt{n}, \quad n = 0,1, \ldots, \tag{1}$$

where $\omega_H = \sqrt{2\omega_c \Delta_0/\hbar}$, $\omega_c = eB/mc$ is the cyclotron frequency and Δ_0 is the maximum superconducting gap. The Dirac-like spectrum of Landau levels arises from the linear dispersion of nodal quasiparticles at zero field. This argumentation neglects the effect of spatially varying supercurrents in the vortex array which were shown to strongly mix individual Landau levels.[21]

Recently, Franz and Tešanović (FT)[12] pointed out that the low-energy quasiparticle states of a $d_{x^2-y^2}$-wave superconductor in a vortex state are most naturally described by strongly dispersive Bloch waves. This conclusion was based on the particular choice of a singular gauge transformation, which allows for the treatment of the uniform external magnetic field and the effects produced by chiral supercurrents on equal footing. The starting point was the Bogoliubov-de Gennes (BdG) equation linearized around a Dirac node. By employing the singular gauge transformation FT mapped the original problem onto that of a Dirac Hamiltonian in periodic vector and scalar potentials, comprised of an array of an effective magnetic Aharonov-Bohm half fluxes, and with a vanishing overall magnetic flux per unit cell. The FT gauge transformation allows use of standard band structure and other zero-field techniques to study the quasiparticle dynamics in the presence of vortex arrays, ordered or disordered. Its utility was illustrated in Ref. 12 through computation of the quasiparticle spectra of a square vortex lattice. A remarkable feature of these spectra is the persistence of the massless Dirac node at finite fields and the appearance of the ''lines of nodes'' in the gap at large values of the anisotropy ratio $\alpha_D = v_F/v_\Delta$, starting at $\alpha_D \simeq 15$. Furthermore, the FT transformation directly reveals that a quasiparticle moving coherently through a vortex array experiences not only a Doppler shift caused by circulating supercurrents but also an *additional*, ''Berry phase'' effect: the latter is a purely quantum mechanical phenomenon and is absent from a typical semiclassical approach. Interestingly, the cyclotron motion in Dirac cones is *entirely* caused by such ''Berry phase'' effect, which takes the form of a half-flux Aharonov-Bohm scattering of quasiparticles by vortices, and does *not* explicitly in-

volve the external magnetic field. It is for this reason that the Dirac-like Landau level quantization is absent from the exact quasiparticle spectrum.

Further progress was achieved by Marinelli, Halperin, and Simon[22] who presented a detailed perturbative analysis of the linearized Hamiltonian of Ref. 12. They showed that the presence of the particle-hole symmetry is of key importance in determining the nature of the spectrum of low-energy excitations. If the vortices are arranged in a Bravais lattice, they showed that, to all orders in perturbation theory, the Dirac node is preserved at finite fields, i.e., the quasiparticle spectrum remains gapless at the Γ point. This result masks intense mixing of individual basis vectors (in the case of Ref. 22 these are Dirac plane waves), including strong mixing of states far removed in energy. The continuing presence of the massless Dirac node at the Γ point after the application of the external field is thus not due to the lack of scattering which is actually remarkably strong. Rather, it is dictated by symmetry: Marinelli *et al.* demonstrated that the crucial agent responsible for the presence of the Dirac node is the particle-hole symmetry, present at every point in the Brillouin zone. The fact that it is the particle-hole symmetry rather than the lack of scattering that protects the Dirac node is clearly revealed in the related problem of a Schrödinger electron in the presence of a single Aharonov-Bohm half-flux, where the density of states acquires a δ function depletion at $\mathbf{k}=0$,[23] thus shifting part of the spectral weight to infinity due to remarkably strong scattering. The authors of Ref. 22 also corrected Ref. 12 by showing that the ''lines of nodes'' must actually be the ''lines of near nodes'' since true zeros of the energy away from Dirac node are prohibited on symmetry grounds. Still, these ''lines'' will act as true nodes in all realistic circumstances, due to extraordinarily small excitation energies.

Marinelli *et al.* also showed that, if the particle-hole symmetry is broken, for example by introducing a non-Bravais vortex lattice with broken inversion symmetry and four vortices in the unit cell, then true lines of nodes can develop for values of anisotropy ratio starting already at $\alpha_D \simeq 5$. They concluded, that the density of states is finite at zero energy and the semiclassical results of Kopnin and Volovik[24] might apply down to zero energy. For a non-Bravais lattice with two vortices per unit cell they found that the quasiparticle spectrum can become gapped.

Very recently Ye[25] discussed transport properties of the quasiparticles described by the Dirac Hamiltonian of Ref. 12 and pointed out some intriguing effects that may take place in random vortex arrays. Also, Altland, Simons, and Zirnbauer investigated general properties of disordered Dirac operators, including vortex disorder.[26]

In this paper we extend the original analysis which was based solely on the *continuum* description by introducing a tight-binding ''regularization'' of the full lattice BdG Hamiltonian, to which we then apply the FT gauge transformation. Our motivation is twofold: First, we have found by explicit numerical computations that different choices of singular gauge transformation result in spectra which, while rather similar, are not the same. Within our numerical accuracy we could not tell whether the spectra have a very slow convergence to the same final result or whether they actually converge to a different answer. This will be discussed again shortly. This problem appears to be a conspiracy between the strong Aharonov-Bohm scattering from magnetic half fluxes which tends to push some states of the unperturbed Hamiltonian to very high energies and the unbounded nature of the Dirac spectrum. It is an interesting issue for future study how to devise the cutoff in the reciprocal lattice sums of the linearized problem which is tailor made for a particular choice of the singular gauge transformation. In this paper, we circumvent this problem entirely by regularizing the original Hamiltonian on a square lattice. The tight-binding formulation regularizes the strong mixing of the basis vectors through the introduction of an upper and a lower bound on the spectrum, thus prohibiting the shift of the spectral weight to infinity.[23] This immediately solves our problem: different choices of singular gauge transformation now rapidly converge to identical spectra, as they should. The low-energy part of the spectrum compares best with the original FT transformation[12] of the linearized Hamiltonian, which might have been expected based on its having the smoothest relative phase between particles and holes.

Second, the lattice formulation allows us to study what, if any, role is played by *internodal* scattering which is simply not a part of the linearized description. We find that under *special* circumstances, when there is a high degree of commensurability between the ionic and vortex lattices, the interference between the nodes can lead to scattering which is surprisingly strong ($\sim\sqrt{B}$) and might be observable in HTS. Such scattering is responsible for opening a gap at the Fermi surface even in the case of a Bravais vortex lattice. In a *typical* situation, however, when the two lattices have a low degree of commensurability or are of different symmetry and particularly when weak thermal or quenched disorder is included, the internodal scattering effectively disappears. We diagonalize the tight-binding Hamiltonian numerically for various order parameter symmetries and both square and triangular vortex lattices. Our treatment provides an access to the entire quasiparticle energy spectrum together with displaying the utility of the FT transformation in analyzing gapped superconductors (e.g. *s*- or p_{x+iy}- wave), which are *a priori* inaccessible through the linearization. We are therefore able to present a unified treatment of a general, both conventional and unconventional, strongly type-II superconducting pairing in the vortex state.

II. BDG HAMILTONIAN AND THE SINGULAR GAUGE TRANSFORMATION: LOW ENERGY PHYSICS OF QUASIPARTICLES AND VORTICES

Because of the nonlocality inherent in the superconductors with higher angular momentum pairing, their Hamiltonians are most naturally formulated on a discrete real space lattice representing the underlying crystalline lattice of the compound in question. Quite generically, the simplest lattice Hamiltonian which allows pairing to occur in *s*-, *p*-, and *d*-wave channels is the tight-binding model with the on-site or nearest neighbor attraction between electrons. Conventional mean-field Hartree-Fock-Bogoliubov decoupling of

the interaction term then leads to the BCS-type lattice Hamiltonian of the form

$$\mathcal{H}=\begin{pmatrix} \hat{h} & \hat{\Delta} \\ \hat{\Delta}^* & -\hat{h}^* \end{pmatrix}, \tag{2}$$

where

$$\hat{h}=-t\sum_{\boldsymbol{\delta}} e^{-i(e/\hbar c)\int_{\mathbf{r}}^{\mathbf{r}+\boldsymbol{\delta}}\mathbf{A}(\mathbf{r})\cdot d\mathbf{l}}\hat{s}_{\boldsymbol{\delta}}-\epsilon_F \tag{3}$$

and

$$\hat{\Delta}=\Delta_0\sum_{\boldsymbol{\delta}} e^{i\phi(\mathbf{r})/2}\hat{\eta}_{\boldsymbol{\delta}}e^{i\phi(\mathbf{r})/2}. \tag{4}$$

The sums are over nearest neighbors and on the square lattice $\delta=\pm\hat{x},\pm\hat{y}$; $\mathbf{A}(\mathbf{r})$ is the vector potential associated with the external magnetic field B, ϵ_F is Fermi energy, and $\hat{s}_{\boldsymbol{\delta}}$ is an operator which is defined by its action on a general function $u(\mathbf{r})$ so that $\hat{s}_{\boldsymbol{\delta}}u(\mathbf{r})=u(\mathbf{r}+\boldsymbol{\delta})$. The operator $\hat{\eta}_{\boldsymbol{\delta}}$ depends on the type of pairing as discussed later.

A quasiparticle wave function is a rank two spinor in the Nambu space, $\psi^T(\mathbf{r})=[u(\mathbf{r}),v(\mathbf{r})]$, and obeys the BdG equation

$$\mathcal{H}\psi=\epsilon\psi. \tag{5}$$

Besides relying on conventional mean-field BCS decoupling, Hamiltonian (2) contains two additional approximations. First, we have assumed that the order-parameter magnitude is constant and equal to Δ_0 everywhere in space. This is essentially the London limit[14] which is expected to be valid in the regime of low fields, $B\ll H_{c2}$, when vortex cores comprise negligible fraction of the sample. Second, we approximated the phase of the order parameter $\phi_{\boldsymbol{\delta}}(\mathbf{r})$, which is a nonlocal field associated with a *bond* between two neighbor sites, by the average of the phases associated with the attached sites,

$$\phi_{\boldsymbol{\delta}}(\mathbf{r})\rightarrow\frac{1}{2}[\phi(\mathbf{r})+\phi(\mathbf{r}+\boldsymbol{\delta})]. \tag{6}$$

This replacement is discussed in more detail in the Appendix A and we expect it to be very accurate far away from the vortex cores where the phase varies slowly, but inadequate in the core. Hamiltonian (2) is therefore useful when considering quasiparticle properties in a dilute vortex lattice, which is the main focus of this work. To study properties of the core region one must explicitly treat the order parameter amplitude variation and nonlocality of its phase as done, e.g., in Refs. 15 and 17. Surprisingly, however, we shall see below that even the present approximation yields results for the core region that are qualitatively correct.

A. Continuum formulation

In many cases our main interest is directed at the long wavelength and low-energy or low-temperature properties. It is precisely in this respect that the quasiparticle excitations in an unconventional superconductor differ most dramatically from its *s*-wave counterpart. Under these circumstances it is desirable to consider a continuum version of the BdG Hamiltonian. For a *d*-wave superconductor such a continuum Hamiltonian was derived by Simon and Lee.[27] It turns out, however, that as written in Ref. 27 this Hamiltonian is not gauge invariant.[28] At fault is the off-diagonal term representing the *d*-wave pairing operator, which does not transform properly under the U(1) gauge group. In Appendix A we have derived the gauge invariant form of this pairing operator for a pure $d_{x^2-y^2}$ superconductor and have outlined how such a derivation can be carried out for other unconventional pairing states. The continuum Hamiltonian reads:

$$\mathcal{H}=\begin{pmatrix} \hat{\mathcal{H}}_e & \hat{\Delta} \\ \hat{\Delta}^* & -\hat{\mathcal{H}}_e^* \end{pmatrix}, \tag{7}$$

with $\hat{\mathcal{H}}_e=1/2m(\mathbf{p}-e/c\mathbf{A})^2-\epsilon_F$ and $\hat{\mathbf{p}}=-i\hbar\nabla$ the momentum operator. If we follow the convention and choose the coordinate axes in the direction of gap nodes the *gauge invariant d*-wave pairing operator has the form

$$\hat{\Delta}=p_F^{-2}\{\hat{p}_x,\{\hat{p}_y,\Delta(\mathbf{r})\}\}+\frac{i}{4}p_F^{-2}\Delta(\mathbf{r})(\hat{p}_x\hat{p}_y\phi), \tag{8}$$

where p_F is the Fermi momentum, ϕ is the phase of the superconducting gap $\Delta(\mathbf{r})$, and curly brackets represent symmetrization, $\{a,b\}=(1/2)(ab+ba)$. The above pairing operator resembles the familiar Simon-Lee form except for the last term which is necessary to restore the full gauge invariance. We emphasize that expression (8) is valid for uniform gap amplitude; otherwise additional terms which involve derivatives of the amplitude appear.

We now use this Hamiltonian as the starting point in our discussion of low-energy quasiparticles in the presence of magnetic field. Operationally, the main difficulty encountered when solving for the eigenstates of Eq. (7) in the vortex state is the nontrivial structure of the order-parameter phase field $\phi(\mathbf{r})$, which is constrained by topology to wind by 2π around the center of each vortex. Ideally, we would want to get rid of this phase to make the problem look as close as possible to the reference solution in which the phase can simply be set to zero. If $\phi(\mathbf{r})$ is a pure gauge, i.e., $\nabla\times\nabla\phi(\mathbf{r})=0$, this is easily accomplished by performing a gauge transformation

$$\mathcal{H}\rightarrow U^{-1}\mathcal{H}U,\quad U=\begin{pmatrix} e^{i\phi(\mathbf{r})/2} & 0 \\ 0 & e^{-i\phi(\mathbf{r})/2} \end{pmatrix}. \tag{9}$$

After this transformation the BdG Hamiltonian becomes

$$\begin{pmatrix} \frac{1}{2m}(\hat{\mathbf{p}}+m\mathbf{v}_s)^2-\epsilon_F & \frac{\Delta_0}{p_F^2}\hat{p}_x\hat{p}_y \\ \frac{\Delta_0}{p_F^2}\hat{p}_x\hat{p}_y & -\frac{1}{2m}(\hat{\mathbf{p}}-m\mathbf{v}_s)^2+\epsilon_F \end{pmatrix},$$

where

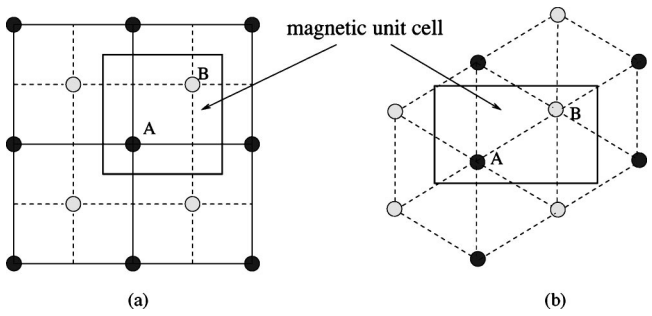

FIG. 1. Example of A and B sublattices for the square (a) and triangular (b) vortex lattice.

$$\mathbf{v}_s(\mathbf{r}) = \frac{1}{m}\left(\frac{\hbar}{2}\nabla\phi - \frac{e}{c}\mathbf{A}\right) \tag{10}$$

is the conventional superfluid velocity. We recognize the term containing $\nabla\phi$ as the Doppler shift of quasiparticles in a locally uniform superflow.[4,5]

However, if $\phi(\mathbf{r})$ contains vortices the situation is far more subtle: the vector field $\nabla\phi(\mathbf{r})$, while still locally uniform, acquires a *global* curvature, i.e.,

$$\nabla\times\nabla\phi(\mathbf{r}) = 2\pi\hat{z}\sum_i \delta(\mathbf{r}-\mathbf{r}_i) \neq 0, \tag{11}$$

where $\{\mathbf{r}_i\}$ denotes vortex positions. Consequently, in the vortex state it is no longer possible to eliminate the superconducting phase by the above transformation (9) and obtain a Hamiltonian describing quasiparticles coupled to the locally uniform superflow. Formally this can be seen from the fact that in the presence of vortices transformation (9) is not single valued. In principle such multiple valuedness of the resulting Hamiltonian could be handled by introducing compensating branch cuts in the quasiparticle wave functions. In practice, however, it is far more desirable to avoid any such complications in the first place.

We follow FT (Ref. 12) and perform a ''bipartite'' singular gauge transformation,

$$\mathcal{H}\rightarrow U^{-1}\mathcal{H}U, \quad U=\begin{pmatrix} e^{i\phi_e(\mathbf{r})} & 0 \\ 0 & e^{-i\phi_h(\mathbf{r})}\end{pmatrix}, \tag{12}$$

where $\phi_e(\mathbf{r})$ and $\phi_h(\mathbf{r})$ are two functions satisfying

$$\phi_e(\mathbf{r}) + \phi_h(\mathbf{r}) = \phi(\mathbf{r}). \tag{13}$$

This more general transformation also eliminates the phase of the order parameter from the pairing term of the Hamiltonian but $\phi_e(\mathbf{r})$ and $\phi_h(\mathbf{r})$ now can be chosen in a way that avoids multiple valuedness and the associated complications. The way to accomplish this is to assign the singular part of the phase field generated by any given vortex to either $\phi_e(\mathbf{r})$ or $\phi_h(\mathbf{r})$, but not both as is done by symmetric transformation (9). Physically, a vortex assigned to $\phi_e(\mathbf{r})$ will be seen by electrons and be invisible to holes, while vortex assigned to $\phi_h(\mathbf{r})$ will be seen by holes and be invisible to electrons.

In practice we implement the above transformation by dividing vortices into two groups A and B, positioned at $\{\mathbf{r}_i^A\}$ and $\{\mathbf{r}_i^B\}$, respectively (see Fig. 1). We then define two phase fields $\phi_A(\mathbf{r})$ and $\phi_B(\mathbf{r})$ such that

$$\nabla\times\nabla\phi_\mu(\mathbf{r}) = 2\pi\hat{z}\sum_i \delta(\mathbf{r}-\mathbf{r}_i^\mu), \quad \mu=A,B, \tag{14}$$

and identify $\phi_e=\phi_A$ and $\phi_h=\phi_B$. Comparison with Eq. (11) confirms that this choice of $\phi_e(\mathbf{r})$ and $\phi_h(\mathbf{r})$ satisfies the condition (13), possibly up to some unimportant nonsingular phase which can be always transformed away by the conventional gauge transformation (9).

The transformed Hamiltonian becomes[29]

$$\begin{pmatrix} \frac{1}{2m}(\hat{\mathbf{p}}+m\mathbf{v}_s^A)^2-\epsilon_F & \hat{D} \\ \hat{D} & -\frac{1}{2m}(\hat{\mathbf{p}}-m\mathbf{v}_s^B)^2+\epsilon_F \end{pmatrix},$$

with $\hat{D}=\Delta_0/2p_F^2[\hat{p}_x+m/2(v_{sx}^A-v_{sx}^B)][\hat{p}_y+m/2(v_{sy}^A-v_{sy}^B)] + (x\leftrightarrow y)$ and

$$\mathbf{v}_s^\mu = \frac{1}{m}\left(\hbar\nabla\phi_\mu - \frac{e}{c}\mathbf{A}\right), \quad \mu=A,B. \tag{15}$$

From the perspective of quasiparticles $\mathbf{v}_s^A$ and $\mathbf{v}_s^B$ can be thought of as *effective* vector potentials acting on electrons and holes, respectively. Corresponding effective magnetic field seen by the quasiparticles is $\mathbf{B}_{\rm eff}^\mu = -mc/e(\nabla\times\mathbf{v}_s^\mu)$, and can be expressed using Eqs. (14) and (15) as

$$\mathbf{B}_{\rm eff}^\mu = \mathbf{B} - \phi_0\hat{z}\sum_i \delta(\mathbf{r}-\mathbf{r}_i^\mu), \quad \mu=A,B, \tag{16}$$

where $\mathbf{B}=\nabla\times\mathbf{A}$ is the physical magnetic field and $\phi_0=hc/e$ is the flux quantum. We observe that quasielectrons and quasiholes propagate in the effective field which consists of (almost) uniform physical magnetic field $\mathbf{B}$ and an array of opposing delta function ''spikes'' of unit fluxes associated with vortex singularities. The latter are different for electrons and holes. As discussed in (Ref. 12) it is desirable to choose A and B vortices in such a way that the effective magnetic field vanishes on average, i.e., $\langle\mathbf{B}_{\rm eff}^\mu\rangle=0$. This translates to a simple requirement that we have precisely one flux spike (of A and B type) per flux quantum of the physical magnetic field. In that case flux quantization guarantees that the right-hand side of Eq. (16) vanishes when averaged over a vortex lattice unit cell containing two physical vortices. It also implies that there must be equal numbers of A and B vortices in the system.

The essential advantage of the choice with vanishing $\langle\mathbf{B}_{\rm eff}^\mu\rangle$ is that $\mathbf{v}_s^A$ and $\mathbf{v}_s^B$ can be chosen periodically in space with periodicity of the magnetic unit cell containing one electronic flux quantum hc/e. Notice that vector potential of a field that does not vanish on average can never be periodic in space. Condition $\langle\mathbf{B}_{\rm eff}^\mu\rangle=0$ is therefore crucial in this respect.

The singular gauge transformation (12) maps the original Hamiltonian of fermionic quasiparticles in finite magnetic field onto a Hamiltonian which is formally in zero average

field and has no singular phase winding in the off-diagonal components. This situation bears some similarity to the fractional quantum Hall effect (FQHE). Here, the composite fermion[30,31] is created by attaching a flux tube to the electron. The details, however, are quite different. In the present case it is the superconducting condensate that creates the fictitious ''flux spikes'' which then on average exactly neutralize the physical applied magnetic field. Unlike in FQHE, the fluxes are stationary and we are generally in the limit where there is a large number of electrons per flux.

To facilitate further insights into the physics of the low-energy quasiparticles we now linearize the transformed Hamiltonian in the vicinity of one of the four nodes of the gap function on the Fermi surface. Following Simon and Lee[27] we obtain $\mathcal{H}_N \simeq \mathcal{H}_0 + \mathcal{H}'$, where

$$\mathcal{H}_0 = \begin{pmatrix} v_F \hat{p}_x & v_\Delta \hat{p}_y \\ v_\Delta \hat{p}_y & -v_F \hat{p}_x \end{pmatrix} \tag{17}$$

is the free Dirac Hamiltonian and

$$\mathcal{H}' = m \begin{pmatrix} v_F v_{sx}^A & \frac{1}{2} v_\Delta (v_{sy}^A - v_{sy}^B) \\ \frac{1}{2} v_\Delta (v_{sy}^A - v_{sy}^B) & v_F v_{sx}^B \end{pmatrix}. \tag{18}$$

Here v_F is the Fermi velocity and $v_\Delta = \Delta_0 / p_F$ denotes the slope of the gap at the node.

$\mathcal{H}_N$ can be viewed as a relativistic Hamiltonian for a $2+1$ massless ''Dirac'' fermion and can be rewritten accordingly as

$$\mathcal{H}_N = v_F (\hat{p}_x + a_x) \tau_3 + v_\Delta (\hat{p}_y + a_y) \tau_1 + m v_F v_{sx}, \tag{19}$$

where τ_i are Pauli matrices, $\mathbf{v}_s = \frac{1}{2}(\mathbf{v}_s^A + \mathbf{v}_s^B) = 1/m(\hbar/2 \nabla \phi - e/c\mathbf{A})$ is the conventional superfluid velocity and $\mathbf{a} = m/2(\mathbf{v}_s^A - \mathbf{v}_s^B) = \hbar/2(\nabla \phi_A - \nabla \phi_B)$ is the internal gauge field. We observe that $\mathbf{v}_s$ couples to the Dirac fermions as a *scalar* potential while $\mathbf{a}$ couples as a *vector* potential. The Dirac ''magnetic field'' $\mathbf{b} = \nabla \times \mathbf{a}$ produced by this vector potential is highly unusual: it consists of delta function spikes located at the vortex centers and it vanishes on average when the numbers of *A* and *B* vortices are equal. Each spike carries precisely one half of the conventional electronic flux quantum ϕ_0 and therefore, although comprising a set of measure zero in the real space, the flux spikes lead to *maximal* Aharonov-Bohm scattering and have strong effect on the quasiparticle spectra. In particular, note that the cyclotron motion in a Dirac cone arises *entirely* through $\mathbf{b} = \nabla \times \mathbf{a}$ and does *not* include explicitly the actual magnetic field $\mathbf{B} = \nabla \times \mathbf{A}$. Such half-flux scattering is a time-reversal invariant and cannot lead to Dirac-like (or any!) Landau level quantization.

B. Internal gauge symmetry

Spectral properties of the continuum linearized Hamiltonian (17) and (18) have been analyzed in great detail[12,22] and initial investigation of its transport properties has been presented.[25] Here we wish to point out a peculiar property of the linearized Hamiltonian as regards the choice of *A* and *B* subsets of vortices, which seems to have been overlooked thus far.

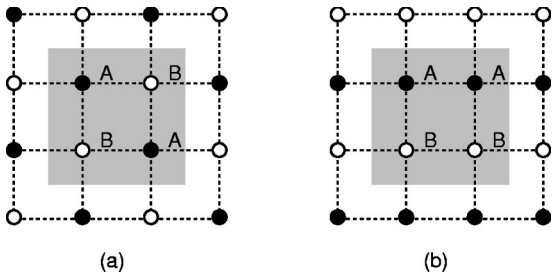

FIG. 2. Two sublattices, ''*ABAB*'' and ''*AABB*'' used to investigate the internal gauge symmetry of the FT transformation. The shaded region marks the unit cell used in the numerical diagonalization.

Logic dictates that all measurable quantities must be independent of our choice of *A* and *B*. This is because there should be no physical distinction between *A* and *B* vortices, the assignment being completely arbitrary. The freedom of assignment of vortices into *A* and *B* subsets represents an internal gauge symmetry of the problem closely related to the fact that electrons condense in pairs and therefore vortices carry *half* of the electronic flux quantum hc/e.

To explicitly test this internal gauge symmetry we have diagonalized the linearized Hamiltonian (17) and (18) using the Bloch wave technique described in Ref. 12 for the two distinct choices of A–B sublattices as illustrated in Fig. 2. We used a unit cell containing 4 vortices in order to be able to compare the band structures for the two cases directly on the same Brillouin zone. The corresponding band structures for the isotropic case ($\alpha_D = v_F / v_\Delta = 1$) are displayed in Fig.

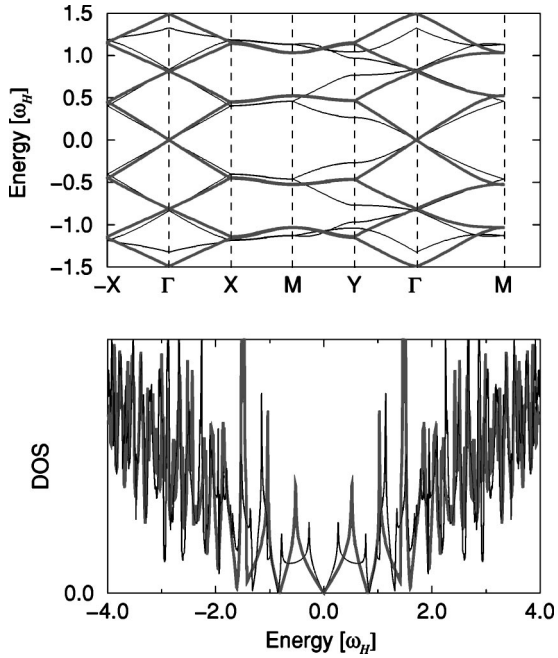

FIG. 3. The band structure (top) and DOS (bottom) of the linearized Hamiltonian with two choices of sublattices: *ABAB* (thick line) and *AABB* (thin line).

3. We observe that although qualitatively similar, their detailed features are *different* and so are the associated densities of states. A similar situation occurs for other values of Dirac cone anisotropy α_D and other symmetries of the vortex lattice, although the case shown in Fig. 3 is an extreme example of the differences. This is a surprising and unexpected result whose ramifications we do not fully understand at the present time.

We expended considerable effort to verify that the difference between the two band structures is not a trivial artifact of our diagonalization procedures. Rather, it appears to be associated with the pathological $\sim r^{-1/2}$ behavior of the Dirac wave functions in the vicinity of a vortex center, which is presumably difficult to mimic using a finite number of Bloch waves which are used as basis states in our numerical diagonalization. We also note that the Aharonov-Bohm scattering induced by the half-flux spikes is extraordinarily strong. As shown by Moroz,[23] in the case of ordinary Schrödinger electron it causes a transfer of spectral weight from zero energy up to infinite energy.

The problem is clearly inherent only to the *linearized* BdG Hamiltonian. In the following Section we show that no such problem arises in the lattice version of the BdG Hamiltonian. This is presumably because the spectrum is bounded (by the tight-binding bandwidth) in this case and therefore all states are accounted for in the numerical diagonalization. Also, the lattice spacing acts as a natural short distance cutoff which regularizes the behavior of the wave functions at the core.

We have also solved the linearized problem by directly discretizing the Hamiltonian (17) and (18) on a square grid in the real space, a technique similar to that described in Ref. 22. The problem persists in this case. We conclude that the problem appears to be caused by a conspiracy between the strong Aharonov-Bohm scattering and the unbounded nature of the Dirac spectrum of Hamiltonian (17) and (18). While we believe that there exists a regularization scheme which would resolve the problem within the linearized formulation, our attempts to construct such a scheme were unsuccessful so far. We leave it as an interesting problem for further investigation.

C. Lattice formulation

It is straightforward to apply the FT singular gauge transformation (12) to the lattice BdG Hamiltonian (2). One obtains

$$\mathcal{H}_N = \begin{pmatrix} -t\sum_{\boldsymbol{\delta}} e^{i\mathcal{V}^A_{\boldsymbol{\delta}}(\mathbf{r})}\hat{s}_{\boldsymbol{\delta}} - \epsilon_F & \Delta_0 \sum_{\boldsymbol{\delta}} e^{-(i/2)\delta\phi}\hat{\eta}_{\boldsymbol{\delta}} e^{(i/2)\delta\phi} \\ \Delta_0 \sum_{\boldsymbol{\delta}} e^{-(i/2)\delta\phi}\hat{\eta}^*_{\boldsymbol{\delta}} e^{(i/2)\delta\phi} & t\sum_{\boldsymbol{\delta}} e^{-i\mathcal{V}^B_{\boldsymbol{\delta}}(\mathbf{r})}\hat{s}_{\boldsymbol{\delta}} + \epsilon_F \end{pmatrix}, \tag{20}$$

where

$$\mathcal{V}^{\mu}_{\boldsymbol{\delta}}(\mathbf{r}) = \int_{\mathbf{r}}^{\mathbf{r}+\boldsymbol{\delta}} \left(\nabla\phi_\mu - \frac{e}{\hbar c}\mathbf{A} \right) \cdot d\mathbf{l}, \quad \mu = A,B, \tag{21}$$

and

$$\delta\phi = \phi_A - \phi_B . \tag{22}$$

We notice that the integrand of Eq. (21) is proportional to the superfluid velocities $\mathbf{v}^{\mu}_s$ defined by Eq. (15) in connection with the continuum Hamiltonian. Appendix B describes an efficient calculation of these quantities in the vortex lattice.

The main benefit of reframing the original problem in this way is the explicit gauge invariance. In the case of a periodic arrangement of vortices the Hamiltonian is periodic with periodicity of a magnetic unit cell containing a pair of A and B vortices. In what follows we consider square and triangular vortex lattices with two physical vortices per unit cell as illustrated in Fig. 1. The vortex center is always placed at the center of the plaquette of the underlying tight-binding lattice.

Following FT we use the familiar Bloch states as the natural basis for finding the eigenvalues of $\mathcal{H}_N$ specified above. In particular we seek the eigensolution of the BdG equation $\mathcal{H}_N\psi = \epsilon\psi$ in the Bloch form

$$\psi_{n\mathbf{k}}(\mathbf{r}) = e^{i\mathbf{k}\cdot\mathbf{r}}\Phi_{n\mathbf{k}}(\mathbf{r}) = e^{i\mathbf{k}\cdot\mathbf{r}} \begin{pmatrix} U_{n\mathbf{k}}(\mathbf{r}) \\ V_{n\mathbf{k}}(\mathbf{r}) \end{pmatrix}, \tag{23}$$

where $(U_{n\mathbf{k}}, V_{n\mathbf{k}})$ are periodic on the corresponding unit cell, n is a band index and $\mathbf{k}$ is a wave vector from the first Brillouin zone. Bloch wave function $\Phi_{n\mathbf{k}}(\mathbf{r})$ satisfies the ''off-diagonal'' Bloch equation $\mathcal{H}_{\mathbf{k}}\Phi_{n\mathbf{k}} = \epsilon_{n\mathbf{k}}\Phi_{n\mathbf{k}}$, with the Hamiltonian of the form $\mathcal{H}_{\mathbf{k}} = e^{-i\mathbf{k}\cdot\mathbf{r}}\mathcal{H}_N e^{i\mathbf{k}\cdot\mathbf{r}}$. In the following section we describe specific forms of such Hamiltonians for the *s*-, *p*-, and *d*-wave symmetries and discuss their solutions.

III. NUMERICAL RESULTS

A. *s*-wave pairing

In the case of *s*-wave pairing the operator $\hat{\eta}_{\boldsymbol{\delta}}$ takes the form $\hat{\eta}_{\boldsymbol{\delta}} = \frac{1}{4}$, and the Hamiltonian simplifies considerably. In particular, the off-diagonal terms become simply Δ_0, and

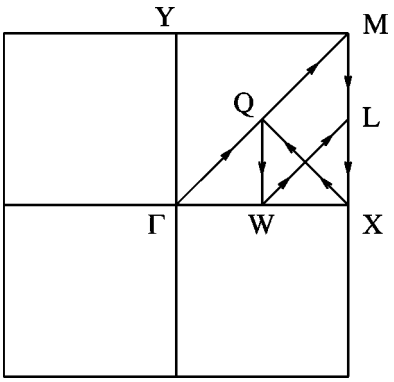

FIG. 4. Magnetic Brillouin zone for the square vortex lattice with the corresponding notations used in the discussion of the quasiparticle band structure.

$$\mathcal{H}_N = \begin{pmatrix} -t\sum_{\boldsymbol{\delta}} e^{i\mathcal{V}^A_{\boldsymbol{\delta}}(\mathbf{r})}\hat{S}_{\boldsymbol{\delta}} - \epsilon_F & \Delta_0 \\ \Delta_0 & t\sum_{\boldsymbol{\delta}} e^{-i\mathcal{V}^B_{\boldsymbol{\delta}}(\mathbf{r})}\hat{S}_{\boldsymbol{\delta}} + \epsilon_F \end{pmatrix}. \tag{24}$$

It is interesting to note that in the limit of high quasiparticle energy, $\epsilon \gg \Delta_0$, the off-diagonal terms become irrelevant, and the equations for the electron and hole part of the Nambu wave function decouple. We recover a Hamiltonian describing holes and electrons in a uniform magnetic field pierced by a lattice of counteracting full Aharonov-Bohm magnetic flux tubes with unit flux quanta hc/e concentrated at the set of point cores. The solution is just the familiar Schrödinger Landau levels, not to be confused with Eq. (1), because the full electronic flux has no effect on the particle energy spectrum.[32] This result is expected from the outset since at high-energies the quasiparticles behave as normal electrons or holes, which know little about the condensate. These high energy quasiparticles experience effectively a uniform magnetic field and move along cyclotron orbits. Similar argument holds for any pairing symmetry and we expect Landau level quantization of the quasiparticle spectrum at energies much larger than Δ_0.

We have numerically diagonalized the above Hamiltonian making use of the standard LAPACK diagonalization routine. We considered a tight-binding lattice of 10×10 sites, which turns out to be sufficiently large to analyze the CdGM regime. The corresponding magnetic field $B=1/(100\delta^2)$ in units of unit flux hc/e per unit area, the superconducting gap $\Delta_0=t$ and the chemical potential $\epsilon_F=-2.2t$ assuring an approximately cylindrical Fermi surface. The resulting spectrum for the Brillouin zone displayed in Fig. 4 and density of states for the square vortex lattice are shown in the Fig. 5. The $B=0$ spectrum has the usual BCS form with a full gap Δ_0. The additional features at $2.1\Delta_0$ and $2.4\Delta_0$ are remnants of the band edge and the van Hove singularity, respectively, present in the normal-state spectrum.

The magnetic field induces low-energy states within the gap, which become localized in the vortex cores. These are CdGM states[13] dispersed into bands. At low energies, the bands are very narrow signaling strong concentration of the wave functions at the vortex cores and insignificant overlaps among the states at neighboring vortices. This fact justifies the chosen parameters. At energies less, but comparable to

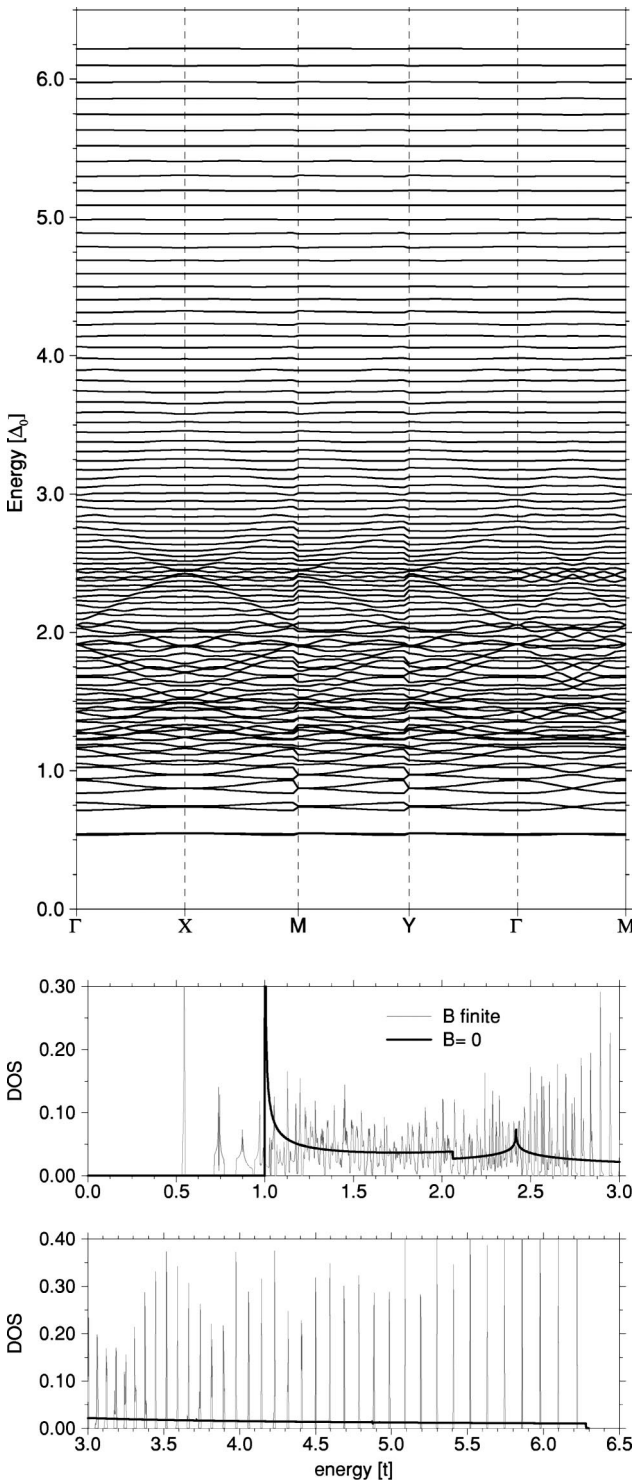

FIG. 5. Top: Quasiparticle band spectrum for an *s*-wave superconductor in the presence of the external magnetic field $B=1/100\delta^2$, and $\Delta_0=t, \epsilon_F=-2.2t$. Bottom: corresponding DOS. Note the bound Caroli-Matricon bands at energies below the gap and the Landau levels at energies $\epsilon \gg \Delta_0$.

Δ_0, the bands are broadened due to increasing overlap among the wave functions. It is interesting to note that CdGM bound states appear despite the fact that our model assumes constant order-parameter amplitude and the effective core size is the tight-binding lattice spacing δ. The small size of the core causes the lowest bound state to be pushed to rather high energy and also that only a few bound states can be resolved with our numerical accuracy. For energies $\epsilon \gg \Delta_0$ the spectrum exhibits Landau level quantization, as expected from the argument presented above.

It is appropriate to illustrate the pitfall lurking in the guise of the symmetric transformation widely used in the literature. At first glance, perhaps the most natural choice for removing the phases from the off-diagonal terms is setting in Eq. (13) $\phi_e(\mathbf{r})=\phi_h(\mathbf{r})=\phi(\mathbf{r})/2$. Note that in this case the transformation

$$U=\begin{pmatrix} e^{i\phi(\mathbf{r})/2} & 0 \\ 0 & e^{-i\phi(\mathbf{r})/2} \end{pmatrix} \tag{25}$$

is not single valued and neither are the resulting wave functions. Nevertheless, ignoring these facts, the Hamiltonian becomes

$$\mathcal{H}_N=\begin{pmatrix} -t\sum_{\boldsymbol{\delta}} e^{i\mathcal{V}_{\boldsymbol{\delta}}(\mathbf{r})}\hat{s}_{\boldsymbol{\delta}}-\epsilon_F & \Delta_0 \\ \Delta_0 & t\sum_{\boldsymbol{\delta}} e^{-i\mathcal{V}_{\boldsymbol{\delta}}(\mathbf{r})}\hat{s}_{\boldsymbol{\delta}}+\epsilon_F \end{pmatrix} \tag{26}$$

with

$$\mathcal{V}_{\boldsymbol{\delta}}(\mathbf{r})=\int_{\mathbf{r}}^{\mathbf{r}+\boldsymbol{\delta}}\left(\frac{1}{2}\nabla\phi-\frac{e}{\hbar c}\mathbf{A}\right)\cdot d\mathbf{l}. \tag{27}$$

In the limit of high quasiparticle energies the equations again decouple, but now they describe a quasiparticle moving in a uniform magnetic field pierced by half electronic flux quanta $hc/2e$ canceling the overall field. These half-fluxes cause significant Aharonov-Bohm scattering and cannot be ignored. As shown in Ref. 32, the spectrum for this problem is *not* that of Landau levels; there is a significant dispersion. Again, this argument is independent of the pairing symmetry.

B. *p*-wave pairing

We follow Matsumoto and Sigrist[8] and for simplicity assume that the prototype *p*-wave superconductor is two dimensional and has a cylindrical Fermi surface. We further assume for simplicity that it is strongly type II, although Sr_2RuO_4 is not of this type. We restrict the Hamiltonian to one of the two degenerate states, p_{x+iy} and ignore the p_{x-iy} part. For p wave (p_x+ip_y) we have

$$\hat{\eta}_{\boldsymbol{\delta}}=\begin{cases} \mp i\hat{s}_{\boldsymbol{\delta}} & \text{if } \boldsymbol{\delta}=\pm\hat{x} \\ \pm\hat{s}_{\boldsymbol{\delta}} & \text{if } \boldsymbol{\delta}=\pm\hat{y}, \end{cases} \tag{28}$$

where $\hat{s}_{\boldsymbol{\delta}}u(\mathbf{r})=u(\mathbf{r}+\boldsymbol{\delta})$. The Hamiltonian becomes

$$\mathcal{H}_N=\begin{pmatrix} -t\sum_{\boldsymbol{\delta}} e^{i\mathcal{V}^A_{\boldsymbol{\delta}}(\mathbf{r})}\hat{s}_{\boldsymbol{\delta}}-\epsilon_F & \Delta_0\sum_{\boldsymbol{\delta}} e^{i\mathcal{A}_{\boldsymbol{\delta}}(\mathbf{r})}\hat{\eta}_{\boldsymbol{\delta}} \\ \Delta_0\sum_{\boldsymbol{\delta}} e^{-i\mathcal{A}_{\boldsymbol{\delta}}(\mathbf{r})}\hat{\eta}^*_{\boldsymbol{\delta}} & t\sum_{\boldsymbol{\delta}} e^{-i\mathcal{V}^B_{\boldsymbol{\delta}}(\mathbf{r})}\hat{s}_{\boldsymbol{\delta}}+\epsilon_F \end{pmatrix}, \tag{29}$$

where the phases $\mathcal{V}^{\mu}_{\boldsymbol{\delta}}(\mathbf{r})$ are defined by Eq. (21) and

$$\mathcal{A}_{\boldsymbol{\delta}}(\mathbf{r})=\frac{1}{2}\int_{\mathbf{r}}^{\mathbf{r}+\boldsymbol{\delta}}(\nabla\phi_A-\nabla\phi_B)\cdot d\mathbf{l}. \tag{30}$$

We chose $\epsilon_F=-2.2t$ which yields approximately circular Fermi surface with the superconducting gap, to a good accuracy, uniform everywhere on the Fermi surface. As in the case of *s* wave, the value of Δ_0 is set equal to t. The resulting spectrum and density of states are shown in the Fig. 6.

The spectrum again reveals bound vortex states broadened into a band. In contrast to the *s*-wave case we now have a state at zero energy. These results are what is expected on the basis of our understanding of a single *p*-wave vortex.[7,8]

C. *d*-wave pairing

To model the high-temperature superconductors such as $YBa_2Cu_3O_7$, we assume that coupling between the Cu-O planes is weak and to the leading approximation can be ignored. On the tight-binding lattice the *d*-wave pairing is given by $\Delta=2\Delta_0[\cos(k_x\delta)-\cos(k_y\delta)]$ which determines the form of the lattice operator to be:

$$\hat{\eta}_{\boldsymbol{\delta}}=\begin{cases} \hat{s}_{\boldsymbol{\delta}} & \text{if } \boldsymbol{\delta}=\pm\hat{x} \\ -\hat{s}_{\boldsymbol{\delta}} & \text{if } \boldsymbol{\delta}=\pm\hat{y}, \end{cases} \tag{31}$$

where as before $\hat{s}_{\boldsymbol{\delta}}u(\mathbf{r})=u(\mathbf{r}+\boldsymbol{\delta})$. With this definition of $\hat{\eta}_{\boldsymbol{\delta}}$ the Hamiltonian for *d*-wave pairing has the same form as Eq. (29).

The results presented in this section correspond to the magnetic field $\phi_0/(1600\delta^2)$ for square vortex lattice and $\phi_0/(1500\delta^2)$ for triangular vortex lattice where $\phi_0=hc/e=4.137\times10^5$ TÅ^2 and δ is the tight-binding lattice constant. Taking $\delta=4$ Å, as in $YBa_2Cu_3O_7$, this corresponds to physical field of 16 T. The above parameters were chosen for computational efficiency, but we did not see any qualitative difference down to the fields as low as $\phi_0/(4900\delta^2)$ corresponding to a magnetic unit cell of $70\delta\times70\delta$ and a field of 5.2 T. Numerical diagonalization was performed using standard ARPACK package routines for sparse matrices. This algorithm provides a set of low-lying eigenvalues and allows handling much larger systems than the full diagonalization used in *s*- and *p*-wave cases.

We find that the quasiparticle wave functions exhibit significant dependence on the symmetry of the vortex lattice. For the square lattice, the overlap among the wave functions corresponding to different nodes is appreciable and there are strong interference effects along the $|x|=|y|$ diagonals, i.e., the directions in the real space where $\Delta(\mathbf{k})$ vanishes. This is illustrated in Fig. 7. For certain commensurability of the tight-binding and the square vortex lattices, the interference

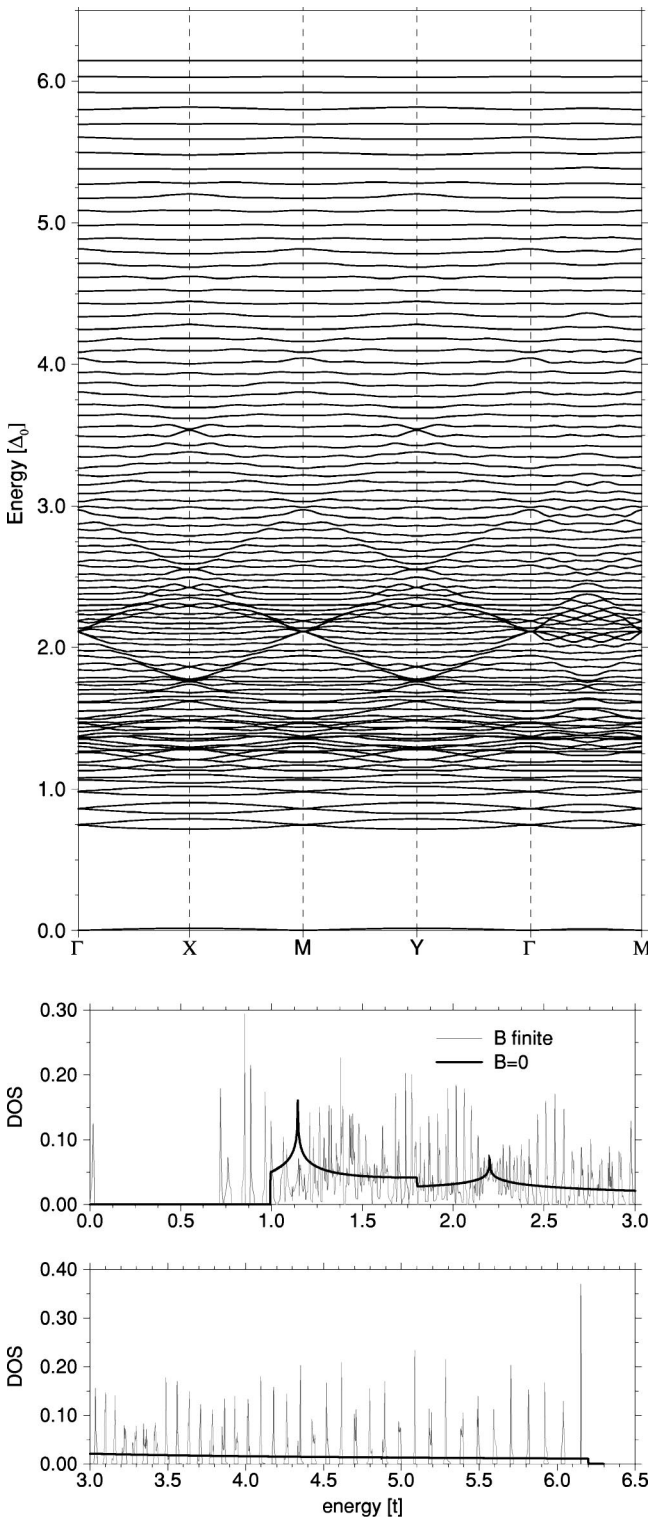

FIG. 6. Top: Quasiparticle band spectrum for a p_{x+iy}-wave superconductor in the presence of the external magnetic field $B=1/100\delta^2$, and $\Delta_0=t, \epsilon_F=-2.2t$. Bottom: The corresponding DOS.

effects are responsible for *opening a gap* at Fermi energy, while for the complementary set of lattices at different commensurability factors, the spectra are gapless at the Dirac Γ point.

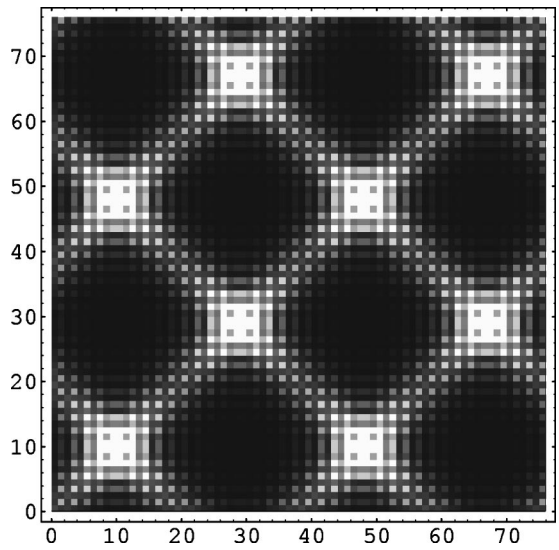

FIG. 7. Local density of states at $E=0$ for the $d_{x^2-y^2}$-wave superconductor with square arrangement of vortices. The plot is in units of the tight-binding lattice constant δ. Bright regions represent maxima while the dark regions represent minima. The parameters are $\epsilon_F=0, \alpha_D=t/\Delta_0=4$. The strong overlaps of the low-energy quasiparticle wave functions along the four nodal directions cause appreciable interference effects which in turn influence the character of the quasiparticle spectrum.

Figures 8 and 9 show the low-energy band structures and the low-energy density of states for the square lattice. The two system sizes shown illustrate the commensurability effect: if the scalar product between the Fermi vector along the nodal direction $\mathbf{k}_F$ and the vortex primitive Bravais lattice vector $\mathbf{d}$ is an even integer times π, the spectrum develops a gap, while it remains gapless if this product is an odd integer times π. The same effect is seen at higher Dirac anisotropy $\alpha_D \equiv t/\Delta_0=10$ (Figs. 10 and 11) and $\alpha_D=15$ (Figs. 12 and 13).

These interference effects persist down to low magnetic fields where the interference gaps scale as $\sim\sqrt{B}$ (see the next section and Fig. 16). In the case of a triangular lattice, the interference effects were greatly reduced (Fig. 14) and no commensurability dependence was observed. We find the spectrum to be gapless at half filling in this case (see Fig. 15).

Finally we note that we have explicitly verified that identical spectra (to within numerical accuracy) are found irrespective of our assignment of the $A-B$ sublattices. This finding confirms that the choice of $A-B$ vortices is an internal gauge symmetry of the problem, as one would expect on general grounds.

IV. DISCUSSION

A. Comparison of continuum and lattice results

The results of Secs. II and III show that, under generic conditions, the spectrum of linearized Dirac Hamiltonian provides a reasonable approximation to the low-energy part of the spectrum of the full BdG Hamiltonian. The Dirac nodes are preserved provided that there is no commensura-

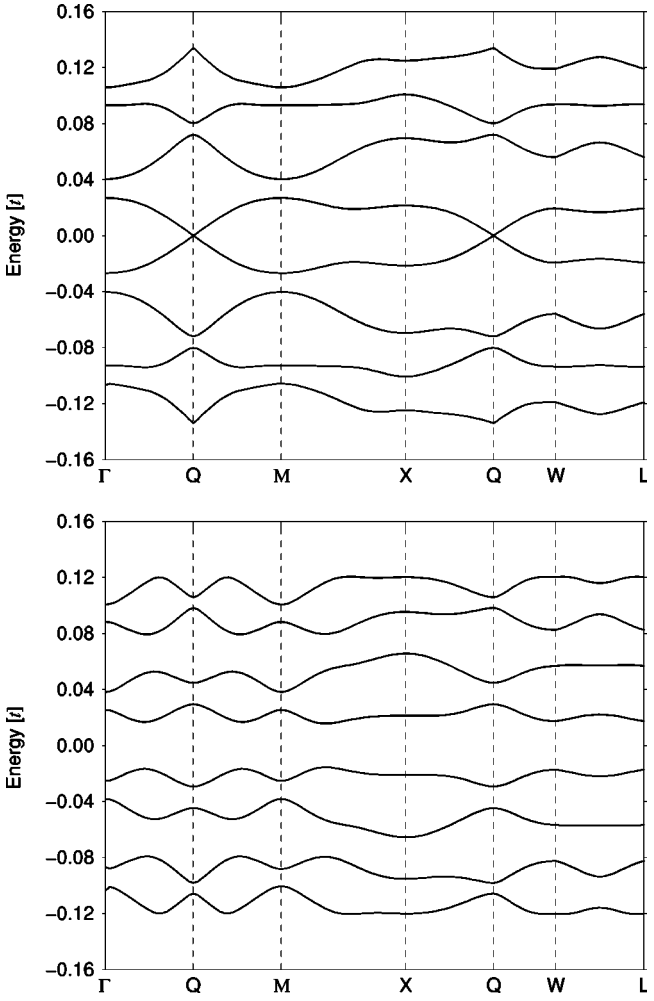

FIG. 8. Low-energy part of the quasiparticle band spectrum for the square vortex lattice. The parameters are $\epsilon_F=0, \alpha_D=4$. Top: example of a gapless spectrum for $l=38\delta$. Note that the node at Q is moved away from the original Dirac Γ point. This effect is a result of a uniform gauge ''boost'' associated with the choice of vortex unit cell and disappears for a unit cell with four vortices. Bottom: example of a gapped spectrum with $l=40\delta$.

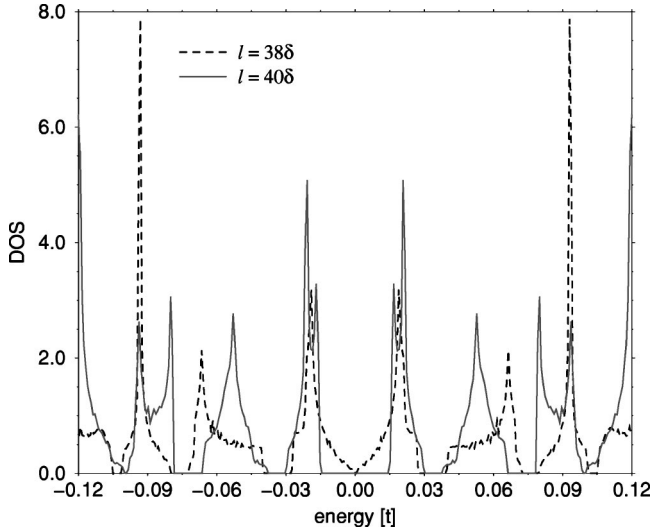

FIG. 9. Low-energy part of the quasiparticle density of states for a $d_{x^2-y^2}$-wave superconductor with square arrangement of vortices for two different interference cases in which $\mathbf{k}_F\cdot\mathbf{d}=2n\pi$ (solid line) and $\mathbf{k}_F\cdot\mathbf{d}=(2n+1)\pi$ (dashed line), n being an integer, $\mathbf{k}_F=(\pi/2,\pi/2)$ a Fermi vector at nodal points, and $\mathbf{d}$ is the primitive vortex lattice vector. Notice the appearance of the gap in the density of states for $\mathbf{k}_F\cdot\mathbf{d}=2n\pi$. Plotted on arbitrary scale, energy is in units of t. The parameters are $\epsilon_F=0, \alpha_D=4$.

tion between $\mathbf{k}_F$ at the node and the primitive vector of the vortex lattice $\mathbf{d}$, and thus the internodal scattering can be neglected. The overall shape of the energy bands is also qualitatively and quantitatively similar for the two cases.

Previous investigations of the linearized Hamiltonian[12,22] established that the spectrum becomes quasi-one-dimensional and lines of nodes appear[33] in the Brillouin zone for large Dirac cone anisotropy $\alpha_D>14$, leading to finite DOS at the Fermi level. Inspection of Fig. 12 suggests that similar effect takes place in the full BdG Hamiltonian, although the one dimensionality is somewhat less pronounced and is restricted to the immediate vicinity of the node. Furthermore, the lines of nodes never quite form (although the tendency is clearly visible along the line $\Gamma\rightarrow M$) and the DOS remains zero at the Fermi level. In the above discussion one needs to bear in mind that the vortex lattice considered here has been rotated by 45° relative to Ref. 12.

B. Scaling of the energy spectrum

The wave function interference effects among the four nodes, which are responsible for opening of the ''interference'' gaps visible in some of our spectra, seem to be in contrast with the results obtained for the linearized Hamiltonian by FT (Ref. 12) and more recently by Marinelli, Halperin, and Simon,[22] where any internodal interaction is ignored and assumed insignificant. Furthermore, Marinelli *et al.* advanced strong analytic arguments that in the presence of particle-hole symmetry the linearized Hamiltonian retains the Dirac node at the Γ point and does not develop a gap to order $\mathcal{O}(l^{-1})$, where l is the magnetic length. We found that the ''interference'' gaps in the quasiparticle spectrum in the case of the square lattice scale with magnetic field as $\sqrt{B}\sim l^{-1}$. This is shown in Fig. 16. The reason for this can be understood from the scaling of the wave functions of the linearized Hamiltonian. We find that there is a $r^{-1/2}$ divergence in the asymptotic solution of the wave function around one vortex. This strong concentration of the wave function around the vortex makes the contribution from the term quadratic in the superfluid velocity particularly enhanced and, independent of regularizing the wave functions to eliminate the divergences at the core, the contribution to the gap is significant. We can then extract the dependence of the wave function on the magnetic length l just from dimensional analysis. The wave function must have units of length^{-1} therefore $\psi\sim(rl)^{-1/2}$. One can see, that the matrix element, and consequently the gaps, will in general scale as l^{-1} for the terms beyond the linearized Hamiltonian. This dependence is extremely difficult to obtain from the plane wave expansion of the wave functions.

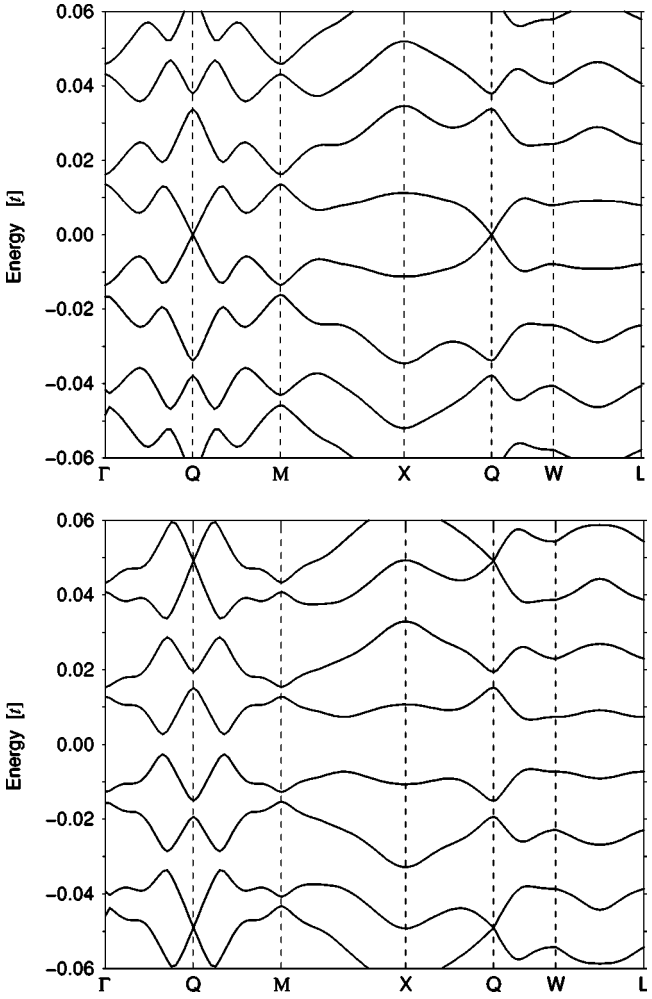

FIG. 10. Low-energy part of the quasiparticle band spectrum for the square vortex lattice. The parameters are $\epsilon_F=0, \alpha_D=10$. Top: gapless spectrum for $l=38\delta$. Note the increase of the dispersion in the QM direction with increase of the Dirac anisotropy α_D. Bottom: gapped spectrum for $l=40\delta$.

Our numerical results strongly suggest that there is a characteristic oscillation in the gap of the spectrum depending on the commensurability of the magnetic lattice and the underlying ionic lattice. This can be interpreted as the internodal scattering. The interaction between the quasiparticles at different nodes is responsible for opening the gaps at the Fermi surface. The effect of the intranodal scattering on these gaps on the Fermi surface is, however, absent since for certain commensurability of the magnetic and ionic lattices there is no gap. Thus we conclude that the effect is purely due to the internodal scattering mediated by the terms beyond the linearized Hamiltonian. The sensitivity of the gaps to the commensurability of the ionic and magnetic lattices is supported by the results with triangular vortex lattice, in which case the spectrum remains gapless as there is no commensurability between ionic and vortex lattice. This supports the view that the internodal scatting alone is responsible for the presence of the gap at the Fermi surface.

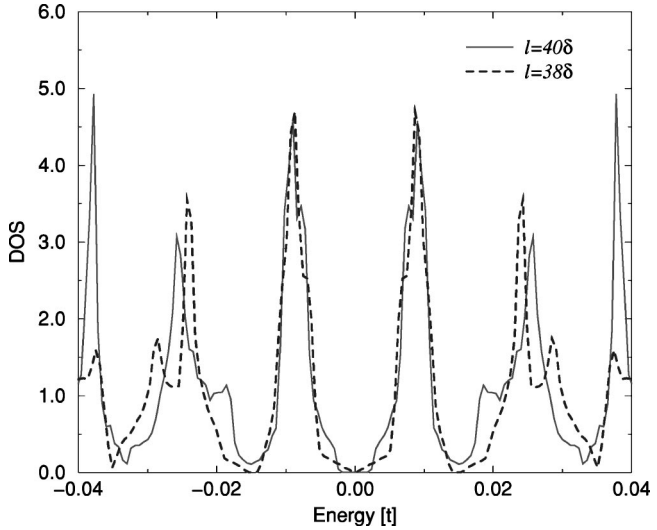

FIG. 11. Low-energy part of the quasiparticle density of states for a $d_{x^2-y^2}$-wave superconductor with square arrangement of vortices for two different interference cases: $l=38\delta$ (dashed) and $l=40\delta$ (solid). Plotted on arbitrary scale, energy is in units of t. The parameters are $\epsilon_F=0, \alpha_D=10$.

C. Comparison with the Doppler-shift-only results for *d*-wave gap

One of the key insights gained from the FT transformation is that the familiar and often used Doppler shift approximation[4,5] is not sufficient to describe the quasiparticle dynamics in the vortex lattice. While the Doppler shift enters at the level of a linearized Dirac Hamiltonian as a periodic *scalar* potential, there is also an effective *vector* potential **a** (Sec. II), which originates from the global curvature of superflow in the presence of vortices. This vector potential term leads to additional strong magnetic half-flux scattering across the whole energy spectrum. It is instructive to compare our results with those obtained by performing the symmetric gauge transformation specified by Eq. (26). As already pointed out the symmetric transformation is *not* single-valued and the resulting transformed Hamiltonian must be accompanied by the branch cuts imposed on its eigenfunctions. If one simply *ignores* these branch cuts altogether, the resulting Hamiltonian contains only the Doppler shift terms and reads

$$\mathcal{H}_S=\begin{pmatrix} -t\sum_{\boldsymbol{\delta}} e^{i\mathcal{V}_{\boldsymbol{\delta}}(\mathbf{r})}\hat{s}_{\boldsymbol{\delta}}-\epsilon_F & \Delta_0\sum_{\boldsymbol{\delta}} \hat{\eta}_{\boldsymbol{\delta}} \\ \Delta_0\sum_{\boldsymbol{\delta}} \hat{\eta}_{\boldsymbol{\delta}} & t\sum_{\boldsymbol{\delta}} e^{-i\mathcal{V}_{\boldsymbol{\delta}}(\mathbf{r})}\hat{s}_{\boldsymbol{\delta}}+\epsilon_F \end{pmatrix}. \tag{32}$$

The density of states obtained by diagonalizing $\mathcal{H}_S$ is shown in Fig. 17. It is significantly different from the results presented in Sec. III. This clearly demonstrates that there is an essential piece of physics missing from the Hamiltonian which contains only the Doppler shift effect, and consequently from a frequently encountered semiclassical approximation to such a Hamiltonian.[4]

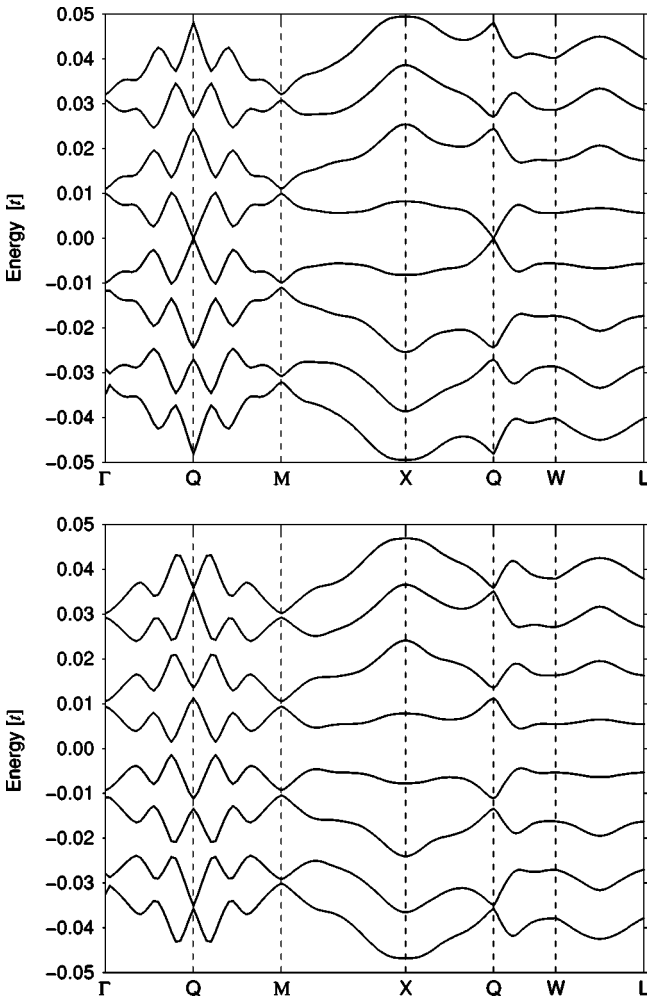

FIG. 12. Low-energy part of the quasiparticle band spectrum for the square vortex lattice. The parameters are $\epsilon_F=0, \alpha_D=15$. Top: gapless spectrum for $l=38\delta$. Note the increase of the dispersion in the QM direction with increase of the Dirac anisotropy α_D. Bottom: gapped spectrum for $l=40\delta$.

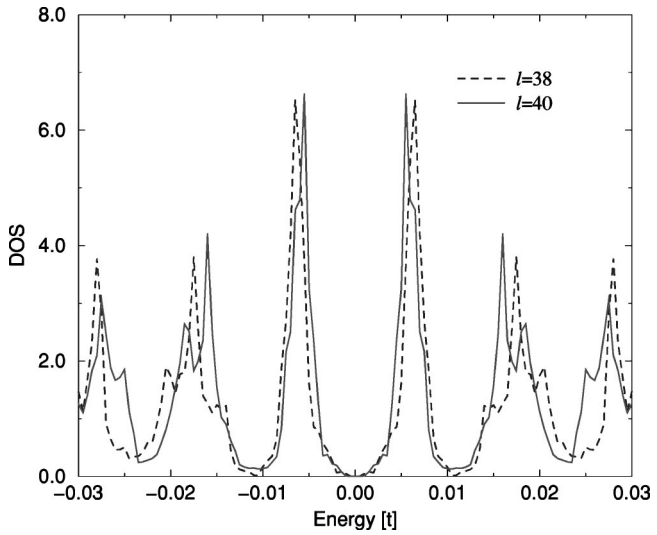

FIG. 13. Low-energy part of the quasiparticle density of states for an $d_{x^2-y^2}$-wave superconductor with square arrangement of vortices for two different interference cases: $l=38\delta$ (dashed) and $l=40\delta$ (solid). Plotted on arbitrary scale, energy is in units of t. The parameters are $\epsilon_F=0, \alpha_D=15$.

V. CONCLUSIONS

In conclusion, the general utility of the singular gauge transformation for the calculation of the quasiparticle spectra in the vortex state of a general pairing symmetry was shown. Once the tight-binding regularization is introduced, the spectrum can be computed in principle exactly using the Bloch states as the natural basis, although one is bound to resort to numerical calculation regardless of respecting the self-consistency. In the case of *s*- and *p*-wave symmetry, we showed that the method applied to an array of vortices leads to results consistent with single vortex solution.

For *d*-wave pairing, the spectrum is also consistent with the single vortex solution from the point of view that all the wave functions are delocalized and no bound states are observed. Additional insight is gained from the exact solution with respect to the continuum linearized version of the theory. For specific commensurability of the tight-binding and square vortex lattice the internodal scattering mediated by the terms neglected in the linearized theory is found to be significant and of the same order of magnitude as the terms present in the linearized Hamiltonian. This is believed to be brought forth by the diverging accumulation of the Dirac wave functions in the vicinity of the vortex core, consequently giving rise to increased significance of the terms beyond linearization. However, since rather special conditions must be met for this effect to be significant, it is suggested that introduction of any perturbing agent such as disorder in the position of the vortices or vortex vibrations will

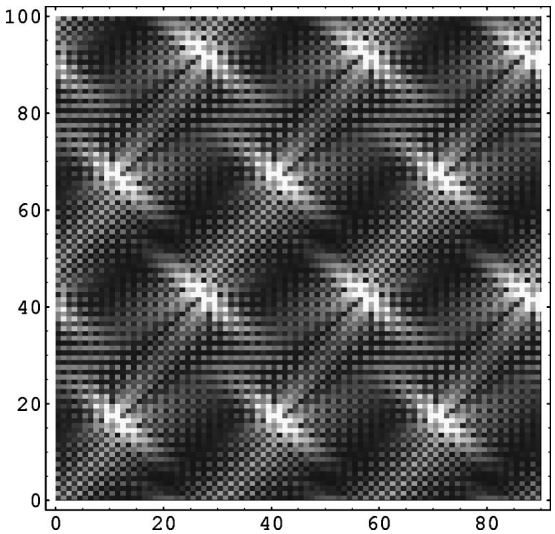

FIG. 14. Displayed is a typical low-energy modulus of a quasiparticle wave function for the $d_{x^2-y^2}$-wave superconductor with triangular arrangement of vortices. The plot is in units of the tight-binding lattice constant δ. Bright regions represent maxima while the dark regions represent minima. The parameters are $\epsilon_F=0, \alpha_D=4$. This plot illustrates the reduction of the interference effects for triangular vortex lattice. As a consequence the gap in the quasiparticle spectrum does not emerge as shown in Fig. 15.

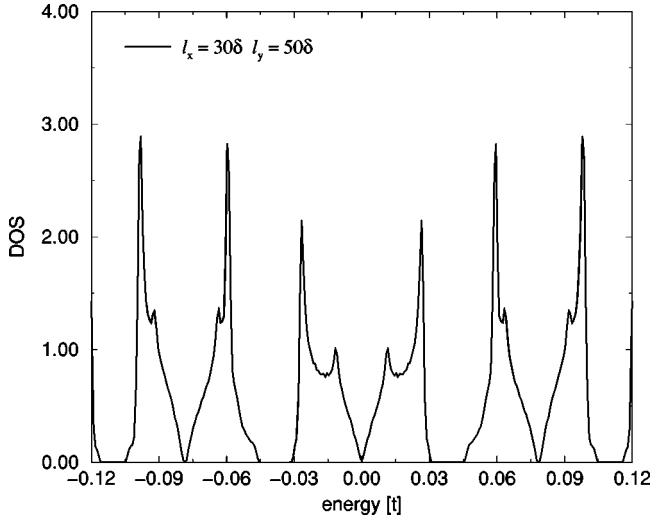

FIG. 15. Low-energy part of the quasiparticle density of states for a *d*-wave superconductor with triangular arrangement of vortices. Plotted on arbitrary scale, energy is in units of *t*. The parameters are $\epsilon_F = 0, \alpha_D = 4$.

lead to decoherence of the matrix elements for the internodal scattering and subsequently to the suppression of the interference effect. It is also possible, and in our view likely, that in a fully self consistent solution the vortex array could spontaneously undergo a slight spatial deformation into an incommensurate state so as to avoid opening gaps in the quasiparticle spectrum. In this respect, at chemical potential $\epsilon_F = 0$, the results of the theory regularized on the tight binding lattice agree with the continuum linearized version.

We have uncovered a peculiar property of the Dirac Hamiltonian: it appears to violate the internal gauge symmetry associated with the assignment of *A* and *B* vortices. Although the final resolution of this apparent contradiction awaits further research, we attribute it tentatively to the unusually strong scattering of Aharonov-Bohm half fluxes acting in the Dirac Hamiltonian with unbounded excitation

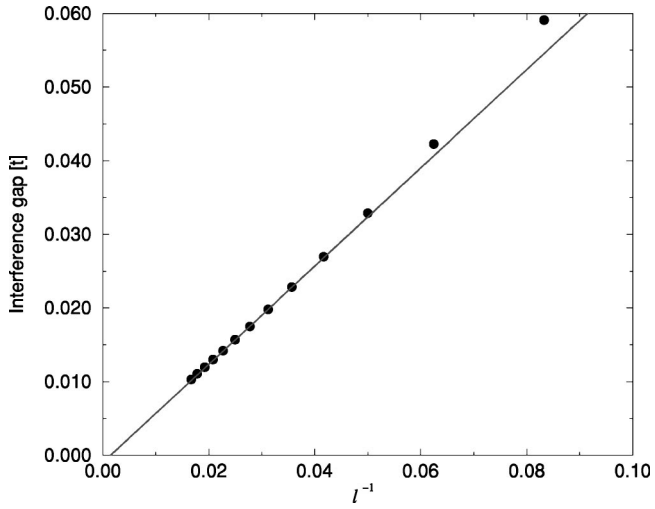

FIG. 16. The magnitude of the interference gaps vs magnetic length *l* exhibits l^{-1} scaling. $\Delta_0 = 0.25t, \epsilon_F = 0$.

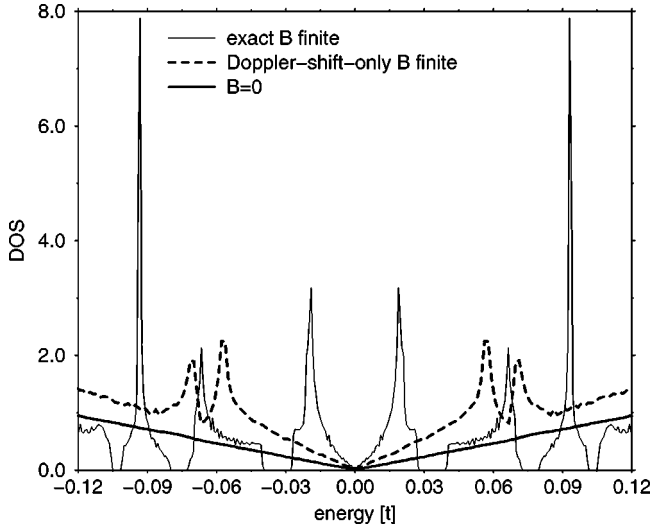

FIG. 17. Comparison of the low-energy part of the quasiparticle density of states for a *d*-wave superconductor with square arrangement of vortices with the DOS obtained from the Doppler-shift-only approximation. Plotted on arbitrary scale, the energy is in units of *t*. The parameters are $\epsilon_F = 0, l = 38\delta, \alpha_D = 4$.

spectrum. This problem does not occur in the full BdG Hamiltonian. We argue that the original ''*ABAB*'' choice of the gauge[12] is the one most representative of the actual spectrum because it results in smoothest possible variation of phase in the vortex lattice. This view is also supported by the direct comparison with the spectrum obtained using the full BdG Hamiltonian.

Number of intriguing issues remain to be addressed. In particular the effect of static and dynamic disorder in vortex positions on the quasiparticle spectra must be understood in order to make connections with the experimental data. Another set of unresolved issues arises in connection with the zero field superconducting state phase-disordered by fluctuating vortex-antivortex pairs.[9–11] One would expect that the ''Berry phase'' term arising from fluctuating vortices would influence in a profound way the critical behavior of the HTS system on the verge of becoming a Mott insulator.

ACKNOWLEDGMENTS

The authors are indebted to B. I. Halperin, L. Marinelli, N. Read, J. Ye, and M. R. Zirnbauer for useful discussions. This research was supported in part by NSF Grant No. DMR-9415549.

APPENDIX A: LATTICE AND CONTINUUM BDG HAMILTONIAN IN A GAUGE INVARIANT FORMULATION

In this Appendix we derive the explicit form of the pairing operator $\hat{\Delta}$ (4) which appears in the lattice BdG Hamiltonian of Eq. (2). We also derive the continuum limit of this operator which is used to construct the BdG equations of Sec. II. Throughout our derivation we pay a special attention to the preservation of local gauge invariance. We start with the general pairing term on a tight-binding square lattice:

$$\sum_{\langle i,j\rangle} \Delta(i,j)[u^*(i)v(j)+u^*(j)v(i)]+\text{H.c.}. \tag{A1}$$

Here $\Delta(i,j)$ is a complex pairing potential defined on the nearest neighbor bonds. Such pairing term generically arises when t–J and related Hamiltonians, which are thought to represent good microscopic models of various unconventional superconductors, are treated within a BCS-type pairing approximation. A conventional *s*-wave case follows from Eq. (A1) if we replace the sum over nearest-neighbor bonds $\langle i,j\rangle$ with the sum over sites i. By construction, the pairing term (A1) is invariant under gauge transformations:

$$\begin{aligned} u(i)&\rightarrow u(i)e^{i\chi(i)},\\ v(i)&\rightarrow v(i)e^{-i\chi(i)},\\ \Delta(i,j)&\rightarrow \Delta(i,j)e^{i\chi(i)+i\chi(j)}, \end{aligned} \tag{A2}$$

where $\chi(i)$ is an arbitrary nonsingular function.

The actual form of the complex function $\Delta(i,j) \equiv D(i,j)\exp[i\varphi(i,j)]$ is obtained as a self-consistent solution of the gap equation in some specific gauge. We denote its ''amplitude'' and phase by $D(i,j)$ and $\varphi(i,j)$, respectively. For convenience, the ''amplitude'' $D(i,j)$ is defined so that it already contains the information about the relative orbital state of a superconductor. For example, in a pure $d_{x^2-y^2}$ superconductor and at zero field, $D(i,j)=-(+)\Delta$ for $\langle i,j\rangle$ in the $x(y)$ direction, where Δ is a complex constant. Furthermore, for the purposes of this paper, we assume that the *actual* amplitude $|\Delta(i,j)|$ can be well approximated by a uniform (real) constant Δ_0, independent of $\langle i,j\rangle$. This assumption is valid in the space between vortices but it clearly breaks down inside a vortex core. At low fields, $H_{c1}\ll H \ll H_{c2}$, where the intervortex separation is much larger than the core size we expect any effect of the inhomogeneous amplitude to be negligibly small.

The essential information about vortex configurations and self-consistent solution at a finite magnetic field is now stored in the bond phase $\varphi(i,j)$. Near a plaquette containing a vortex $\varphi(i,j)$ changes rapidly from bond to bond. Far from vortex cores, however, we expect $\varphi(i,j)$ to be some smoothly varying function undergoing only small changes between neighboring bonds. Consequently, in the regions far away from vortex cores we can replace the *bond* phase $\varphi(i,j)$ by a suitably chosen *site* phase variables $\phi(i)$. The natural choice for the $\phi(i)$'s is a simple average:

$$e^{i\phi(i)}=\frac{1}{4}\sum_{\sigma} e^{i\varphi(i,i+\sigma)}, \tag{A3}$$

where the sum over σ runs over four bonds containing the site i. With this choice of $\phi(i)$'s we can replace:

$$e^{i\varphi(i,j)}\rightarrow e^{i[\phi(i)+\phi(j)]/2}. \tag{A4}$$

Note that, given the choice of site variables (A3), Eq. (A4) is an approximation, accurate up to second-order lattice derivatives of $\phi(i)$'s. We could use a more elaborate representation of $\varphi(i,j)$'s in terms of $\phi(i)$'s so that Eq. (A4) is satisfied to even higher degree of accuracy. This, however, is entirely unnecessary in the present context, since our overall accuracy is precisely at the level represented by Eqs. (A3) and (A4). The replacement (A4) simplifies the pairing term of the lattice BdG Hamiltonian and reproduces the form of the pairing operator $\hat{\Delta}$ (4) used in our lattice Hamiltonian of Eq. (2).

The above replacement of bond phases $\varphi(i,j)$'s with site phases $\phi(i)$'s is also a necessary first step in our derivation of the continuum BdG Hamiltonian. Since both $u(i)$ and $v(i)$ appearing in Eq. (A1) are site fields we expect that the continuum pairing term in unconventional superconductors will involve $u(\mathbf{r})$ and $v(\mathbf{r})$ acted upon by some *local* operator. To determine the explicit form of this operator we first combine Eqs. (A1) and (A3) into:

$$\begin{aligned} \frac{1}{2}\sum_i e^{i\phi(i)}\sum_{\sigma} D(i,i+\sigma)e^{i\varphi(i,i+\sigma)-i\phi(i)}\\ \times[u^*(i)v(i+\sigma)+u^*(i+\sigma)v(i)]+\text{H.c.}, \end{aligned} \tag{A5}$$

where we have transformed the summation over bonds into the summation over sites. We now use $\varphi(i,i+\sigma)=\frac{1}{2}\phi(i)+\frac{1}{2}\phi(i+\sigma)+\mathcal{O}(\delta^2\phi)$, Eq. (A4) where δ^2 denotes second-order lattice derivatives which are unimportant in the continuum limit. Also, from now on we restrict our attention to the most interesting case, a pure $d_{x^2-y^2}$ superconductor. This allows us to rewrite Eq. (A5) as:

$$\begin{aligned} \frac{1}{2}\sum_i \Delta(i)\{&-e^{i\phi(i+\hat{\mathbf{x}})/2-i\phi(i)/2}[u^*(i)v(i+\hat{\mathbf{x}})+u^*(i+\hat{\mathbf{x}})v(i)]\\ &-e^{i\phi(i-\hat{\mathbf{x}})/2-i\phi(i)/2}[u^*(i)v(i-\hat{\mathbf{x}})+u^*(i-\hat{\mathbf{x}})v(i)]\\ &+e^{i\phi(i+\hat{\mathbf{y}})/2-i\phi(i)/2}[u^*(i)v(i+\hat{\mathbf{y}})+u^*(i+\hat{\mathbf{y}})v(i)]\\ &+e^{i\phi(i-\hat{\mathbf{y}})/2-i\phi(i)/2}[u^*(i)v(i-\hat{\mathbf{y}})\\ &+u^*(i-\hat{\mathbf{y}})v(i)]\}+\text{H.c.}, \end{aligned} \tag{A6}$$

where $\Delta(i)\equiv\Delta\exp[i\phi(i)]$ and $\hat{\mathbf{x}},\hat{\mathbf{y}}$ are unit displacements on the square lattice. Next, we expand

$$\begin{aligned} e^{i\phi(i\pm\hat{\mathbf{x}}(\hat{\mathbf{y}}))/2-i\phi(i)/2}\approx 1+\frac{i}{2}\{\phi(i\pm\hat{\mathbf{x}}(\hat{\mathbf{y}}))-\phi(i)\}\\ -\frac{1}{8}\{\phi(i\pm\hat{\mathbf{x}}(\hat{\mathbf{y}}))-\phi(i)\}^2+\cdots, \end{aligned} \tag{A7}$$

make a transition to continuum variables $u(i)\rightarrow a u(\mathbf{r})$, $v(i)\rightarrow a v(\mathbf{r})$, $\Delta(i)\rightarrow\Delta(\mathbf{r})$, $\phi(i)\rightarrow\phi(\mathbf{r})$, $\Sigma_i\rightarrow\int(d^2r/a^2)$, and use the standard definitions of lattice derivatives to finally obtain the continuum version of the pairing term:

$$\frac{-a^2}{2}\int d^2r\Big\{u^*(\mathbf{r})\Delta(\mathbf{r})\Big[\Big(\partial_x+\frac{i}{2}(\partial_x\phi(\mathbf{r}))\Big)\times\Big(\partial_x+\frac{i}{2}(\partial_x\phi(\mathbf{r}))\Big)v(\mathbf{r})\Big]+\Big[\Big(\partial_x+\frac{i}{2}(\partial_x\phi(\mathbf{r}))\Big)\times\Big(\partial_x+\frac{i}{2}(\partial_x\phi(\mathbf{r}))\Big)u^*(\mathbf{r})\Big]\Delta(\mathbf{r})v(\mathbf{r})-(x\to y)\Big\}+\text{H.c.} \tag{A8}$$

In going from Eqs. (A6) to (A8) one encounters some lengthy but straightforward algebra. We found that decomposing the sum over nearest neighbors in Eq. (A6) into *s*-, *p*-, and *d*-wave components relative to site *i* facilitates the bookkeeping and makes the computations rather efficient. All the relevant derivatives up to and including second order are kept and accounted for. Higher-order derivatives do not appear reflecting of our original starting point of the nearest-neighbor pairing of only Eq. (A1). Note that a is the lattice spacing in our model.

The form of the local continuum pairing operator is now apparent. We can view $\Delta(\mathbf{r})=\Delta\exp[i\phi(\mathbf{r})]$ as representing the *center-of-mass* portion of the gap function. The original nonlocality, arising from the *relative* $d_{x^2-y^2}$ character of the pairing, manifests itself through ''covariant'' derivatives $\partial_{\mathbf{r}}+i/2[\partial_{\mathbf{r}}\phi(\mathbf{r})]$, where $\phi(\mathbf{r})$ is precisely the phase of $\Delta(\mathbf{r})$. Note that Eq. (A8) is explicitly invariant under the continuum version of local gauge transformations: $u(\mathbf{r})\to u(\mathbf{r})\exp[i\chi(\mathbf{r})]$, $v(\mathbf{r})\to v(\mathbf{r})\exp[-i\chi(\mathbf{r})]$, $\Delta(\mathbf{r})\to\Delta(\mathbf{r})\exp[2i\chi(\mathbf{r})]$.

The off-diagonal elements of the Hamiltonian matrix appearing in the continuum BdG equations are obtained by taking the functional derivatives of Eq. (A8) with respect to $u^*(\mathbf{r})$ and $v(\mathbf{r})$. This results in:

$$-a^2\{\partial_x,\{\partial_x,\Delta(\mathbf{r})\}\}+a^2\{\partial_y,\{\partial_y,\Delta(\mathbf{r})\}\}-\frac{i}{4}\Delta(\mathbf{r})a^2[(\partial_x^2\phi)-(\partial_y^2\phi)], \tag{A9}$$

and its Hermitian conjugate. Here we used the standard notation: $\{\hat{a},\hat{b}\}\equiv\frac{1}{2}(\hat{a}\hat{b}+\hat{b}\hat{a})$. In performing the functional derivatives we have exploited the fact that all spatial dependence of $\Delta(\mathbf{r})$ comes through its phase, i.e., $\partial_{\mathbf{r}}\Delta(\mathbf{r})=i\Delta(\mathbf{r})\partial_{\mathbf{r}}\phi(\mathbf{r})$, in line with our previous assumptions.

While our derivation starts with a familiar model of the lattice *d*-wave superconductor (A1) and naturally describes the $d_{x^2-y^2}$ state in actual continuum calculations it is often more convenient to consider a d_{xy} superconductor, so that either an x or a y axis coincides with a particular nodal direction, as in Sec. II. We can obtain the pairing term in the continuum BdG Hamiltonian of a d_{xy} superconductor by simply rotating our result (A8) by 45°:

$$\frac{-a^2}{2}\int d^2r\Big\{u^*(\mathbf{r})\Delta(\mathbf{r})\Big[\Big(\partial_x+\frac{i}{2}(\partial_x\phi(\mathbf{r}))\Big)\times\Big(\partial_y+\frac{i}{2}(\partial_y\phi(\mathbf{r}))\Big)v(\mathbf{r})\Big]+\Big[\Big(\partial_x+\frac{i}{2}(\partial_x\phi(\mathbf{r}))\Big)\times\Big(\partial_y+\frac{i}{2}(\partial_y\phi(\mathbf{r}))\Big)u^*(\mathbf{r})\Big]\Delta(\mathbf{r})v(\mathbf{r})+(x\to y)\Big\}+\text{H.c.} \tag{A10}$$

Similarly, by taking functional derivatives we obtain the off-diagonal matrix elements of the continuum BdG Hamiltonian operator:

$$-a^2\{\partial_x\{\partial_y,\Delta(\mathbf{r})\}\}-a^2\{\partial_y,\{\partial_x,\Delta(\mathbf{r})\}\}-\frac{i}{2}\Delta(\mathbf{r})a^2(\partial_x\partial_y\phi), \tag{A11}$$

and its Hermitian conjugate, which is precisely the expression used in Sec. II, provided that we identify p_F^{-2} with $2a^2$.

The above derivation can be easily repeated for a *p*-wave lattice Hamiltonian and is in fact only simpler. We therefore do not give it explicitly but trust that the *d*-wave derivation provides a sufficiently detailed prescription. Similarly, our derivation is straightforwardly generalized to other unconventional forms of superconducting pairing.

APPENDIX B: PHASE FACTORS AND SUPERFLUID VELOCITIES

In this Appendix we derive expressions for superfluid velocities $\mathbf{v}_s^A$ and $\mathbf{v}_s^B$ which enter both continuum and lattice versions of the BdG Hamiltonians in consideration in Sec. II. We start by taking the curl of Eq. (15),

$$\nabla\times\mathbf{v}_s^{\mu}=\frac{2\pi\hbar}{m}\Big[\hat{z}\sum_i\ \delta(\mathbf{r}-\mathbf{r}_i^{\mu})-\mathbf{B}/\phi_0\Big], \tag{B1}$$

where $\phi_0=hc/e$ is the flux quantum, $\mathbf{B}=\nabla\times\mathbf{A}$, and we have used Eq. (14). In the intermediate field regime the magnetic field distribution is to an excellent approximation described by the conventional London equation,[14]

$$\mathbf{B}-\lambda^2\nabla^2\mathbf{B}=\frac{1}{2}\phi_0\hat{z}\sum_i\ \delta(\mathbf{r}-\mathbf{r}_i), \tag{B2}$$

where λ is the London penetration depth and the sum now runs over all vortex positions. The London equation is easily solved by going over to the Fourier space, obtaining $\mathbf{B}(\mathbf{r})=(2\pi)^{-2}\int d^2k e^{i\mathbf{k}\cdot\mathbf{r}}\mathbf{B}_{\mathbf{k}}$ with

$$\mathbf{B}_{\mathbf{k}}=\frac{1}{2}\phi_0\hat{z}\frac{\sum_i e^{-i\mathbf{k}\cdot\mathbf{r}_i}}{1+\lambda^2k^2}. \tag{B3}$$

If we now Fourier transform Eq. (B1) we obtain

$$i\mathbf{k}\times\mathbf{v}^{\mu}_{s\mathbf{k}}=\frac{2\pi\hbar}{m}\left[\hat{z}\sum_i e^{-i\mathbf{k}\cdot\mathbf{r}_i}-\mathbf{B}_{\mathbf{k}}/\phi_0\right]. \tag{B4}$$

To solve for $\mathbf{v}^{\mu}_{s\mathbf{k}}$ we take a vector product of both sides with $i\mathbf{k}$. After substituting for $\mathbf{B}_{\mathbf{k}}$ and some easy algebra we may express

$$\mathbf{v}^{A}_{s}=\frac{2\pi\hbar}{m}\int\frac{d^2k}{(2\pi)^2}\frac{i\mathbf{k}\times\hat{z}}{k^2}\left(A_{\mathbf{k}}-\frac{1}{2}\frac{A_{\mathbf{k}}+B_{\mathbf{k}}}{1+\lambda^2k^2}\right)e^{i\mathbf{k}\cdot\mathbf{r}}, \tag{B5}$$

and a similar expression for $\mathbf{v}^{B}_{s}$ with $A_{\mathbf{k}}$ and $B_{\mathbf{k}}$ interchanged. Here we have defined

$$A_{\mathbf{k}}=\sum_i e^{-i\mathbf{k}\cdot\mathbf{r}^A_i},\quad B_{\mathbf{k}}=\sum_i e^{-i\mathbf{k}\cdot\mathbf{r}^B_i}.$$

Equation (B5) gives an explicit formula for $\mathbf{v}^{\mu}_{s}$ which can be evaluated for arbitrary distribution of vortices. For strongly type-II materials in fields well above H_{c1} Eq. (B5) may be simplified further by rewriting the expression in the brackets as

$$A_{\mathbf{k}}\frac{\lambda^2k^2}{1+\lambda^2k^2}-\frac{1}{2}\frac{B_{\mathbf{k}}-A_{\mathbf{k}}}{1+\lambda^2k^2},$$

and noting that since $\lambda^2k^2\sim\lambda^2/d^2\gg1$ (d being intervortex distance), the second term can be safely neglected. We thus obtain

$$\mathbf{v}^{\mu}_{s}=\frac{2\pi\hbar\lambda^2}{m}\int\frac{d^2k}{(2\pi)^2}\frac{i\mathbf{k}\times\hat{z}}{1+\lambda^2k^2}\sum_i e^{i\mathbf{k}\cdot(\mathbf{r}-\mathbf{r}^{\mu}_i)}, \tag{B6}$$

a formula used in Ref. 12 which is valid for all practical purposes. Phase factors $\mathcal{V}$ and $\mathcal{A}$ entering the lattice Hamiltonians of Sec. III may be obtained by simple line integrals of Eq. (B6).

*Present address: Department of Physics and Astronomy, University of British Columbia, Vancouver, BC, Canada V6T 1Z1.

[1] D. J. Van Harlingen, Rev. Mod. Phys. **67**, 515 (1995).
[2] P. A. Lee, Science **277**, 50 (1997).
[3] See, e.g., W.A. Atkinson, P.J. Hirschfeld, A.H. MacDonald, and K. Ziegler, cond-mat/0005487 (unpublished), and references therein.
[4] G. E. Volovik, Pis'ma Zh. Éksp. Teor. Fiz. **58**, 457 (1993) [JETP Lett. **58**, 469 (1993)].
[5] S. K. Yip and J. A. Sauls, Phys. Rev. Lett. **69**, 2264 (1992).
[6] T. M. Rice, Nature (London) **396**, 627 (1998); K. Ishida, H. Mukuda, Y. Kitaoka, Nature (London) **396**, 658 (1998).
[7] G. E. Volovik, cond-mat/9709159; JETP Lett. **70**, 609 (1999).
[8] M. Matsumoto and M. Sigrist, J. Phys. Soc. Jpn. **68**, 724 (1999); Physica B **281**, 973 (2000).
[9] M. Franz and A. J. Millis, Phys. Rev. B **58**, 14 572 (1998).
[10] H.-J. Kwon and A. T. Dorsey, Phys. Rev. B **59**, 6438 (1999).
[11] L. Balents, M. P. A. Fisher, and C. Nayak, Phys. Rev. B **60**, 1654 (1999).
[12] M. Franz and Z. Tešanović, Phys. Rev. Lett. **84**, 554 (2000).
[13] C. Caroli, P.G. de Gennes, and J. Matricon, Phys. Lett. **9A**, 307 (1964).
[14] P. G. de Gennes, *Superconductivity of Metals and Alloys* (Addison-Wesley, Reading, 1989).
[15] M. Franz and Z. Tešanović, Phys. Rev. Lett. **80**, 4763 (1998).
[16] X. R. Resende and A. H. MacDonald, Bull. Am. Phys. Soc. **43**, 573 (1998).
[17] Y. Wang and A. H. MacDonald, Phys. Rev. B **52**, R3876 (1995).
[18] K. Yasui and T. Kita, Phys. Rev. Lett. **83**, 4168 (1999).
[19] L. P. Gor'kov and J. R. Schrieffer, Phys. Rev. Lett. **80**, 3360 (1998).
[20] P. W. Anderson, cond-mat/9812063 (unpublished).
[21] A. S. Melnikov, J. Phys.: Condens. Matter **82**, 4703 (1999).
[22] L. Marinelli, B. I. Halperin, and S. H. Simon, Phys. Rev. B **62**, 3488 (2000).
[23] A. Moroz, Phys. Rev. A **53**, 669 (1996).
[24] N. B. Kopnin and G. E. Volovik, Pis'ma Zh. Éksp. Teor. Fiz. **64**, 641 (1996) [JETP Lett. **64**, 690 (1996)].
[25] J. Ye, cond-mat/0003251 (unpublished).
[26] A. Altland, B. D. Simons, and M. R. Zirnbauer, cond-mat/0006362 (unpublished).
[27] S. H. Simon and P. A. Lee, Phys. Rev. Lett. **78**, 1548 (1997).
[28] We are grateful to J. Ye and N. Read for alerting us to this fact. We also thank N. Read for an in-depth discussion of the issue of gauge invariance of effective Hamiltonians.
[29] We note that with the correct form of the pairing operator (8) this result is now exact. In Ref. 12 it was necessary to neglect spurious higher order derivative terms which appeared as a consequence of the lack of the gauge invariance.
[30] J. K. Jain, Phys. Rev. Lett. **63**, 199 (1989).
[31] B. I. Halperin, P. A. Lee, and N. Read, Phys. Rev. B **47**, 7312 (1993).
[32] M. Nielsen and P. Hedegård, Phys. Rev. B **51**, 7679 (1995).
[33] Marinelli *et al.* (Ref. 22) argued based on symmetry that there can be no true lines of nodes in the Brillouin zone. Even so, our numerical investigation indicates that the small gap that exists in the linearized model closes up rapidly as α_D increases and becomes numerically indistinguishable from zero above $\alpha_D\approx18$. For all practical purposes one may therefore speak about ''lines of nodes'' in this context.